Nonexocytotic serotonin release tonically suppresses serotonergic neuron activity

Boris Mlinar, Alberto Montalbano, Gilda Baccini, Francesca Tatini, Rolando Berlinguer Palmini, and Renato Corradetti

Department of Neuroscience, Psychology, Drug Research and Child Health, University of Florence, 50121 Florence, Italy

The firing activity of serotonergic neurons in raphe nuclei is regulated by negative feedback exerted by extracellular serotonin $(5\text{-HT})_o$ acting through somatodendritic 5-HT1A autoreceptors. The steady-state $[5\text{-HT}]_o$, sensed by 5-HT1A autoreceptors, is determined by the balance between the rates of 5-HT release and reuptake. Although it is well established that reuptake of 5-HT_o is mediated by 5-HT transporters (SERT), the release mechanism has remained unclear. It is also unclear how selective 5-HT reuptake inhibitor (SSRI) antidepressants increase the $[5\text{-HT}]_o$ in raphe nuclei and suppress serotonergic neuron activity, thereby potentially diminishing their own therapeutic effect. Using an electrophysiological approach in a slice preparation, we show that, in the dorsal raphe nucleus (DRN), continuous nonexocytotic 5-HT release is responsible for suppression of phenylephrine-facilitated serotonergic neuron firing under basal conditions as well as for autoinhibition induced by SSRI application. By using 5-HT1A autoreceptor-activated G protein–gated inwardly rectifying potassium channels of patched serotonergic neurons as 5-HT_o sensors, we show substantial nonexocytotic 5-HT release under conditions of abolished firing activity, Ca^{2+} influx, vesicular monoamine transporter 2–mediated vesicular accumulation of 5-HT, and SERT-mediated 5-HT transport. Our results reveal a cytosolic origin of 5-HT_o in the DRN and suggest that 5-HT_o may be supplied by simple diffusion across the plasma membrane, primarily from the dense network of neurites of serotonergic neurons surrounding the cell bodies. These findings indicate that the serotonergic system does not function as a sum of independently acting neurons but as a highly interdependent neuronal network, characterized by a shared neurotransmitter pool and the regulation of firing activity by an interneuronal, yet activity-independent, nonexocytotic mechanism.

INTRODUCTION

The brain ascending serotonergic system plays a key role in a broad range of behaviors, and its dysfunction has been implicated in the pathogenesis of psychiatric disorders, most notably depression, anxiety disorders, and obsessive–compulsive disorder. In mammals, the dorsal raphe nucleus (DRN) contains about half of the brain's serotonergic neurons, the axons of which innervate most of the forebrain. Serotonergic neurons in the DRN display slow and regular action potential–firing activity proportional to the level of behavioral activation across the sleep–wake–arousal cycle (Jacobs and Azmitia, 1992). The serotonergic tone in projection areas is regulated by negative feedback of serotonin $(5\text{-HT})_o$

exerted locally through the activation of axonal 5-HT1B autoreceptors and indirectly through suppression of firing activity by activation of somatodendritic 5-HT1A autoreceptors in raphe nuclei (Sharp et al., 1989; Riad et al., 2000; Crespi, 2009). The 5-HT1A autoreceptor-mediated suppression of serotonergic neuron firing that we refer to as autoinhibition is of particular interest because it can control the entire serotonergic system. The level of functional expression of 5-HT1A autoreceptors influences a range of 5-HT–dependent brain functions such as amygdala-mediated emotional response (Fisher et al., 2006; Fakra et al., 2009), formation and display of social defeat (Cooper et al., 2008), autonomic regulation (Audero et al., 2008; Baccini et al., 2012), depressive endophenotype and responsiveness to antidepressant drugs (Richardson-Jones et al., 2010), and aggression (Audero et al., 2013). Despite numerous studies on 5-HT1A autoreceptors, the physiological mechanism of autoinhibition remains elusive (Albert et al., 2011; Altieri et al., 2013). Specifically, the subcellular 5-HT pool from which basal 5-HT_o originates, as

The Rockefeller University Press $30.00
J. Gen. Physiol. Vol. 145 No. 3   225–251
www.jgp.org/cgi/doi/10.1085/jgp.201411330

225

well as the nature of its release, has remained unresolved (Piñeyro and Blier, 1999; Adell et al., 2002). For example, studies in which the 5-HT_o level in the DRN was directly measured with microdialysis in vivo have produced contradictory results, suggesting both that basal 5-HT_o originates from the cytoplasmic pool and does not depend on serotonergic neuron firing activity (Adell et al., 1993), and that 5-HT_o originates from action potential–dependent exocytotic release (Matos et al., 1996; Portas et al., 1996; Tao et al., 1997). In the median raphe, microdialysis studies indicated exocytotic 5-HT release, although tonic activation of 5-HT1A autoreceptors was not detected under basal conditions (Bosker et al., 1994, 1996; Adell and Artigas, 1998). Finally, the mechanism by which selective 5-HT reuptake inhibitor (SSRI) treatment increases $[5\text{-HT}]_o$ in raphe nuclei has also remained unresolved (Albert et al., 2011) despite being of considerable interest, as it has been hypothesized that autoinhibition caused by the increase in $[5\text{-HT}]_o$ delays the therapeutic effect of SSRIs (Artigas et al., 1996).

Axons and dendrites of serotonergic neurons are abundant in raphe nuclei, although with a low rate of varicosities and synaptic specializations (Descarries et al., 1982; Park et al., 1982). In some species, serotonergic neuron dendrites form conspicuous structures (Felten and Harrigan, 1980; Park et al., 1982) or contain vesicles (Chazal and Ralston, 1987) expressing vesicular monoamine transporter 2 (VMAT2; Colgan et al., 2012). Accordingly, electrochemical detection of 5-HT_o has shown that evoked serotonergic transmission in the DRN has characteristics of paracrine rather than classic, hardwired synaptic transmission (Bunin and Wightman, 1998; Bunin et al., 1998). Early functional studies have suggested that 5-HT release in raphe nuclei might occur by canonical, impulse-dependent axonal exocytosis as well as by somatodendritic exocytosis or dendrodendritic inhibition (Hery et al., 1982; Wang and Aghajanian, 1982). Subsequently, serotonergic inhibitory postsynaptic potentials were recorded from serotonergic neurons (Yoshimura and Higashi, 1985; Williams et al., 1988; Pan et al., 1989), and it is now assumed that 5-HT release from axonal collaterals causes autoinhibition (Albert et al., 2011; Altieri et al., 2013). In addition, it was recently demonstrated that depolarization and glutamate receptor activation produce somatodendritic 5-HT exocytosis (De Kock et al., 2006; Kaushalya et al., 2008; Colgan et al., 2009, 2012). These studies have shown multiple ways to induce 5-HT release in raphe nuclei, but their involvement in autoinhibition has remained undefined. On the other hand, electrophysiological studies in vivo (Fornal et al., 1996; Hajós et al., 2001; Haddjeri et al., 2004) and in brain slices (Liu et al., 2005; Mlinar et al., 2005; Evans et al., 2008) have revealed that basal 5-HT_o tonically activates 5-HT1A autoreceptors in the DRN in the absence of external stimulation, raising the possibility

that autoinhibition is mediated by a different mechanism than stimulation-evoked 5-HT release. Here, by using an electrophysiological approach, we show that autoinhibition of serotonergic neurons in the DRN is caused by continuous, activity-independent nonexocytotic 5-HT release, originating primarily from surrounding neurites.

MATERIALS AND METHODS

All animal manipulations were performed according to the European Community guidelines for animal care (DL 116/92, application of the European Communities Council Directive 86/609/EEC) and were approved by the Committee for Animal Care and Experimental Use of the University of Florence. Male Wistar rats were purchased from Harlan Italy. Tryptophan hydroxylase-2 knockout ($Tph2^{-/-}$) mice (Gutknecht et al., 2012) were obtained from K.P. Lesch (University of Würzburg, Würzburg, Germany). After weaning, animals were housed in groups of three to five per cage and maintained under standard laboratory conditions (food and water ad libitum, 12 12-h light–dark cycle with lights on from 08:00 to 20:00, ambient temperature at $22 \pm 1°C$, and relative humidity of 40–50%). Animals (3–10 wk of age at the experimental day) were anesthetized with isoflurane (ether in early experiments) and decapitated. The brain was rapidly removed and dissected in ice-cold gassed (95% O_2 and 5% CO_2) artificial cerebrospinal fluid (ACSF) composed of (mM): 124 NaCl, 2.75 KCl, 1.25 NaH_2PO_4, 1.3 $MgCl_2$, 2 $CaCl_2$, 26 $NaHCO_3$, and 11 D-glucose. The brainstem was sliced coronally into 250–400-µm-thick slices with a vibratome (DSK T1000; Dosaka). After recovery for at least 2 h at room temperature, the slices were individually transferred to the recording chamber and superfused continuously with warmed ACSF at a rate of ~2 ml min^{-1}. Slices were allowed to equilibrate for at least 30 min before the beginning of the recording. Drugs were bath-applied through either peristaltic pump– or a gravity-driven perfusion system, and a complete exchange of the recording chamber volume occurred in ~1 min. Neurons within DRN were visualized by infrared differential interference contrast (IR-DIC) video microscopy with a Newicon camera (C2400-07; Hamamatsu) mounted on an upright microscope (Axioskop; Carl Zeiss). Recordings were made using an amplifier (EPC-10; HEKA). Data were analyzed using Patchmaster 2 (HEKA), Clampfit 9.2 (Molecular Devices), and Prism 5 software (GraphPad Software). Patch pipettes were prepared from thick-walled borosilicate glass on an electrode puller (P-97 Brown-Flaming; Sutter Instrument).

Loose-seal cell-attached recordings

Action potential–firing activity of serotonergic neurons was recorded by loose-seal cell-attached recordings on 350–400-µm-thick slices from 80–200-g rats, at a temperature of 34–36°C. To reproduce the noradrenergic drive that facilitates serotonergic neuron firing during wakefulness in slices (Levine and Jacobs, 1992), ACSF was supplemented with the α_1 agonist phenylephrine (10 µM) (Vandermaelen and Aghajanian, 1983). In some experiments, glutamatergic and GABAergic synaptic transmission was inhibited by supplementing ACSF with the cocktail of blockers as in whole-cell recording. The pipette solution for cell-attached recordings contained (mM): 125 NaCl, 10 HEPES, 2.75 KCl, 2 $CaCl_2$, and 1.3 $MgCl_2$, pH 7.4 with NaOH. Loose-seal cell-attached recordings (5–20-MΩ seal resistance; 3–6-MΩ pipette resistance) were acquired continuously in voltage-clamp mode with pipette potential maintained at 0 mV. Signals were filtered at 3 kHz and digitized at 10 kHz. The firing rate was reported using 10-s bins. Recordings were aborted if firing frequency was sensitive to changes in pipette holding potential or if shape of action

current changed. Because experiments in this study depended on endogenous 5-HT, recordings were done from neurons located at least 40 µm below the slice surface (Mlinar et al., 2005). Most recorded neurons were located in the dorsal and ventromedial part of the DRN. Neurons were identified according to electrophysiological criteria (Vandermaelen and Aghajanian, 1983; Allers and Sharp, 2003). Neurons were presumed to be serotonergic when, during at least a 5-min-long control period at the beginning of the recording, they displayed a slow (<5 Hz) and steady (coefficient of variation of instantaneous frequency, <20%) firing rate; asymmetric action current (ratio of upstroke to downstroke amplitude, >3.5) with a long peak-to-peak interval (>1.2 ms, proportional to action potential half-height width). Only neurons with a stable baseline firing rate were used. Neurons having a firing rate of <0.8 Hz in phenylephrine-supplemented ACSF were not used because they typically had unstable baseline activity and often ceased to discharge action potentials.

In experiments in which pharmacological treatments caused obvious reduction or cessation of the spiking activity toward the end of the recordings, slices were perfused with 20–100 nM of the selective 5-HT1A receptor antagonist, Way-100635 (N-(2-(-4 (2-methoxyphenyl)-1-piperazinyl)ethyl)-N-(2-pyridinyl) cyclohexane carboxamide) for 10–15 min to ensure that the observed effect was caused by a $[5\text{-HT}]_o$ increase. Experiments in which Way-100635 failed to recover the firing rate to at least 90% of the predrug level were discarded. In control experiments, done in the absence of pharmacological treatments, bath application of 100 nM Way-100635 for 15 min did not change the firing rate ($-6.7 \pm 8.9\%$; mean $\pm$ SD; $n = 9$). In some experiments, Way-100635 was substituted with 150 µM of G protein–gated inwardly rectifying potassium (GIRK) channel blocker, Ba^{2+} ($BaCl_2$) for 5–7 min. Alternatively, at the end of recordings in which the firing rate did not substantially change in response to the experimental protocol, response to 5-HT1A receptor agonists R(+)-8-hydroxy-2-(di-n-propylamino)tetralin (R-8-OH-DPAT; 30 nM) or 5-carboxamidotryptamine maleate (5-CT; 10 nM) were tested, and neurons in which firing was not abolished ($n = 3$) were deemed unhealthy or nonserotonergic and excluded from analyses. In some loose-seal cell-attached recordings, drugs were focally applied using PicoSpritzer III (General Valve Operation). For focal application, drugs were dissolved in the pipette solution used for cell-attached recordings and filled into a small-bore tip pipette (R_{pip} of ≈6.8–8.2 MΩ). The pipette was positioned under IR-DIC, and drugs were ejected from the pipette tip by long pulses using minimal pressure (4.5–9 kPa) sufficient to produce small tissue displacement as visualized with the microscope.

Single-unit extracellular recordings
In early experiments, the firing rate was recorded by conventional single-unit extracellular method using a submerged-type chamber in which the slice was superfused on both surfaces. Recordings were made with glass microelectrodes filled with 150 mM NaCl and a resistance of 12–15 MΩ. Single-unit potentials were passed through a high input impedance amplifier (NL 102G; Digitimer) and filters (band-pass 50 Hz to 5 or 10 kHz). The resulting signal was digitized via Digidata 1200 (Axon Instruments) to a PC controlled by Clampex 8 (Axon Instruments) in a gap-free acquisition mode.

Whole-cell voltage-clamp recordings of GIRK current
Whole-cell recordings were done at 28–30°C from 250–300-µM-thick slices of 3–5-wk-old animals. To block synaptic transmission, in whole-cell experiments ACSF was supplemented with a cocktail of glutamate and GABA receptor blockers consisting of: 10 µM NBQX (2,3-dioxo-6-nitro-1,2,3,4-tetrahydrobenzo[f]quinoxaline-7-sulfonamide disodium salt), 20 µM DAPV (D-(-)-2-amino-5-phosphonopentanoic acid), 10 mM strychnine hydrochloride,

10 µM SR-95531 (6-imino-3-(4-methoxyphenyl)-1(6H)-pyridazinebutanoic acid hydrobromide), and 2 µM CGP-55845 (3-N[1-(S)-(3,4-dichlorophenyl)ethyl]

amino-2-(S)-hydroxypropyl-P-benzyl-phosphinic acid hydrochloride). The pipette solution consisted of (mM): 120 K gluconate, 15 KCl, 2 $MgCl_2$, 10 HEPES, 0.1 EGTA, 10 Na_2-phosphocreatine, 4 MgATP, and 0.3 Na_3-GTP, pH 7.35 with KOH. Pipettes had a resistance of 2–5 MΩ. After establishing whole-cell recording configuration, serotonergic neurons were identified on the basis of electrophysiological properties displayed in current-clamp mode (Li et al., 2001): action potential half-height width of >1.5 ms; absence of fast afterhyperpolarization; absence of depolarizing sag in response to hyperpolarizing pulse (from $-60/-65$ to $-110/-120$ mV); and maximal sustained firing rate of <12 Hz (in response to long depolarizing current pulses). The identity of most of the recorded neurons was pharmacologically confirmed as serotonergic during the normal course of the experiment as they, contrary to nonserotonergic neurons in the DRN, showed prominent 5-HT1A receptor-activated GIRK current. Alternatively, at the end of the recording, the serotonergic identity of neurons was confirmed by activation of GIRK conductance of >3 nS in response to bath application of 5-HT1A receptor agonists R-8-OH-DPAT (30 nM) or 5-CT (10–30 nM). In these experiments, we used an extracellular solution containing 5.5 mM K^+ (the additional 2.75 mM by Na^+ substitution) to increase the driving force for inward K^+ current and to shift K^+ reversal potential to a more positive value, permitting reliable detection of inwardly rectifying K^+ currents. Under these conditions, serotonergic neurons displayed a linear current–voltage relationship at membrane potentials negative to -85 mV, where essentially all the ionic current (apart from the seal leak) was being carried through GIRK channels when activated by 5-HT1A autoreceptors. We used hyperpolarizing voltage ramps from the holding potential of -65 mV (to -125 mV, every 10 s; 100 mV s^{-1}; 3-kHz cutoff frequency low-pass filter; 10-kHz sampling frequency) and measured the conductance from the slope of inward K^+ current in range from -110 to -90 mV ($G_{-110/-90mV}$). To monitor access resistance throughout the recording, hyperpolarizing pulses (10 mV; 100-ms duration; 16-kHz low-pass filter; 25-kHz sampling frequency; cell capacitance cancellation circuit switched off) were interlaced with ramps. This protocol permitted stable recording and reliable $G_{-110/-90mV}$ measurement for at least 40 min and in some cases for more than 1 h, with the exception of experiments in Ca^{2+}-free extracellular solution, in which ohmic leak started developing after 20–30 min of stable recording. To calculate net 5-HT1A autoreceptor-activated GIRK current ($I_{5\text{-HT1A}}$) and conductance ($G_{5\text{-HT1A}}$) present during a recording, the 5-HT1A autoreceptor-insensitive current was measured at the end of a recording after the application of 20–50 nM of the selective 5-HT1A receptor antagonist Way-100635 for 10–15 min and subtracted from the total current.

Estimation of $[5\text{-HT}]_o$ from 5-HT1A autoreceptor-activated GIRK conductance
5-HT1A autoreceptor-activated GIRK conductance can be used as a 5-HT_o sensor. The detection range of the sensor is determined by concentration dependence for 5-HT activation of the 5-HT1A autoreceptor. Although calibration of the sensor with known concentrations of 5-HT is impractical in situ because of poor penetration of 5-HT into DRN slice preparations (Williams et al., 1988; Mlinar et al., 2005), the useful range of the sensor can be estimated on the basis of 5-HT concentration–response for $I_{5\text{-HT1A}}$ activation calculated by using acutely isolated serotonergic neurons, a preparation uncompromised by 5-HT reuptake and metabolism. Based on such a calculated EC_{50} of 30 nM for 5-HT and unitary Hill's slope (Penington et al., 1993), 10–90% of the GIRK conductance activation would correspond to $[5\text{-HT}]_o$ of 3.3–270 nM, with near-linear proportionality for concentrations in the

10–100-nM range. Because the basal $[5\text{-HT}]_o$ in vivo is 10 nM, as measured by voltammetry (Crespi et al., 1988), and the basal $[5\text{-HT}]_o$ under conditions in this study was expectedly slightly lower, both basal and elevated $[5\text{-HT}]_o$ should be within the range of the 5-HT1A–GIRK sensor. Furthermore, based on the EC_{50} of 30 nM for 5-HT, the $[5\text{-HT}]_o$ can be estimated from $G_{5\text{-HT1A}}$ if the zero value of $G_{5\text{-HT1A}}$ is determined in response to the application of Way-100635, and the maximal $G_{5\text{-HT1A}}$ is calculated as the difference in $G_{-110/-90mV}$ recorded in the presence of a maximally active concentration of a 5-HT1A receptor full agonist (e.g., 100 nM R-8-OH-DPAT or 30 nM 5-CT) and $G_{-110/-90mV}$ recorded in the presence of Way-100635. To precisely estimate the $[5\text{-HT}]_o$, the maximal and zero $G_{5\text{-HT1A}}$ should be determined for each recorded neuron. Because in this study it was important to obtain a reliable zero $G_{5\text{-HT1A}}$ value, Way-100635 was applied at the end of all recordings, but maximal $G_{-110/-90mV}$ was determined only in a few experiments. For example, in the recording shown in Fig. 8 (A and B), calculated $G_{5\text{-HT1A}}$ was 2.33 nS in citalopram, 7.47 nS in citalopram plus L-tryptophan (Trp), and 11.32 nS in 30 nM 5-CT, corresponding to $[5\text{-HT}]_o$ of 7.8 and 58 nM in citalopram and citalopram plus Trp, respectively. For the rest of the experiments, we can only approximate $[5\text{-HT}]_o$ by using the mean maximal $G_{5\text{-HT1A}}$ value of 6.22 nS (SD of 2.27 nS; range of 3.31 to 11.32 nS; $n = 22$), determined in response to the application of 30 nM 5-CT in experiments done under the same conditions (5.5 mM $[K^+]_o$). Based on the standard concentration–response curve, with the maximal $G_{5\text{-HT1A}}$ value of 6.22 nS and unitary Hill's slope, the change of 1 nS corresponds to the change of ~31 nM in $[5\text{-HT}]_o$ for recorded $G_{5\text{-HT1A}}$ within the range from ~1.1 to 5.1 nS.

Rationale for the choice of 5-HT concentrations intracellularly applied through the recording pipette

To examine 5-HT efflux from an individual serotonergic neuron, 5-HT was included in the pipette solution. The concentration of 5-HT in the cytosol of serotonergic neurons is in dynamic equilibrium, set by multiple variables, i.e., precursor availability, rates of synthesis and degradation, release, reuptake, and packaging into vesicles. Because the exact concentration of 5-HT normally present in the cytosol of mammalian serotonergic neurons is unknown, we used 5-HT at concentrations of 0.3 and 3 mM, assumed to be one to two orders of magnitude higher than normal, based on the following reasoning: (a) The upper limit of cytosolic 5-HT concentration in serotonergic neuron cell bodies is likely determined by monoamine oxidase type B (MAOB), which has a K_m of ~1.2 mM for 5-HT (Fowler and Tipton, 1982). In our conditions, block of MAOB by deprenyl caused only a weak reduction in the firing rate (~14%; 1–10 µM; 60 min; $n = 10$; not depicted), suggesting that cytosolic 5-HT is in a low micromolar range, well below MAOB K_m value. (b) Considering an extracellular concentration of 10 nM 5-HT in raphe (Crespi et al., 1988), vesicular 5-HT concentration of ~270 to ≥400 mM (Bruns et al., 2000; Balaji et al., 2005) and concentration gradients reachable by SERT (Adams and DeFelice, 2002) and VMAT2 (Schuldiner et al., 1995) of $\geq 10^3$ and $>10^4$, respectively, cytosolic 5-HT can be assumed to be ~10–40 µM. (c) An intracellular 5-HT concentration of ~50–380 µM was measured in large invertebrate serotonergic cells (Fuller et al., 1998; Hatcher et al., 2008). The cytosolic 5-HT concentration is expectedly lower because these measures include vesicular 5-HT, and it was estimated that ~26 and ~17% of total 5-HT somatic content is packaged into secretory vesicles in rat serotonergic neurons (Colgan et al., 2009) and in differentiated RN46A cells (Balaji et al., 2005), respectively. We thus assume that 300 µM 5-HT is at the upper limit of physiologically attainable cytosolic 5-HT concentration.

Whole-cell recording of serotonergic postsynaptic responses

Serotonergic synaptic responses were recorded in the same conditions as GIRK current except for the following differences:

(a) in extracellular solution, $[K^+]_o$ was 2.75 mM instead of 5.5 mM, and NBQX was substituted with 20 µM DNQX (6,7-dinitroquinoxaline-2,3-dione disodium salt); (b) in most of the experiments, the pipette solution contained no EGTA, and K-gluconate was substituted with KCH_3SO_3; and (c) slice thickness was 300–350 µm. The whole-cell configuration was obtained, and the identity of neurons as serotonergic or nonserotonergic was established in current-clamp mode. To examine postsynaptic serotonergic responses in the DRN nonserotonergic neurons, smaller neurons (Descarries et al., 1982) (capacitance of 10–30 pF) were targeted for the recording. Neurons were considered nonserotonergic when they had an action potential half-height width of 0.5–1.0 ms. Additional distinguishing characteristics of nonserotonergic neurons in whole-cell recordings were: fast afterhyperpolarization after action potentials (in most cases); depolarizing sag in response to hyperpolarizing pulse (from $-60/-65$ to $-110/-120$ mV for 1 s; in most cases 10–15 mV); maximal sustained firing rate of >20 Hz, in response to 3-s-long depolarizing current pulses; and the absence or sometimes small <1 nS of GIRK conductance activation in response to the application of 5-HT1A receptor agonists (30 nM R-8-OH-DPAT or 10–30 nM 5-CT). In a few cases in which the identity of the recorded neurons appeared ambiguous at the beginning of the recording, the recording was interrupted. After cell-type identification, neurons were kept at the resting membrane potential in voltage follower mode, or, more often, held at -60 mV in voltage-clamp mode. To evoke serotonergic postsynaptic responses, slices were stimulated by bipolar-stimulating electrodes using a constant voltage simulator (DS2 Isolated Stimulator, Digitimer). We typically used one concentric bipolar electrode (125-µm diameter; Platinum-Iridium; CBARC75; FHC Inc.) placed 50–300 µm (mostly 200–250 µm) from the recording neuron and one large twisted bipolar electrode (Ni-Cr–insulated wires; 70-µm OD; interpolar distance of 100–110 µm; homemade) placed at a different angle at the distance of 300–750 µm from the neuron. Stimulating electrodes were positioned away from the recording neuron dendrites. The second stimulation electrode was used if stimulation with the first one failed to evoke serotonergic postsynaptic response. A stimulation attempt was considered unsuccessful when: (a) stimuli of increasing intensity did not evoke postsynaptic responses bigger than 0.5 pA (or 0.5 mV in current-clamp mode) but, at the same intensity, evoked a direct (nonsynaptic) electrical response in the recording cell; or (b) stimulation reached tissue damage intensity level (40–50 V; 200–500-µs duration). In addition, because a subpopulation of serotonergic neurons in vivo fires doublets and short bursts of action potentials (Hajós et al., 1995), in some of experiments where single stimuli were ineffective, we additionally tried to evoke 5-HT–mediated inhibitory postsynaptic currents ($IPSC_{5\text{-HT}}$) with a train of five stimuli (5–50 Hz), although this resulted in no detectable $IPSC_{5\text{-HT}}$ in all attempts in serotonergic ($n = 26$) and nonserotonergic ($n = 8$) neurons. When serotonergic postsynaptic responses were evoked, recording proceeded with neurons held at -60 mV, and stimuli (200-µs duration) with intensity set to evoke full response were delivered at an interstimulus interval of 30 s. Higher stimulation frequencies were not used, as they produced decay of serotonergic synaptic responses.

HPLC determination of 5-HT content in brainstem slices

The 5-HT content in raphe nuclei–containing brainstem slices was determined as described previously (Mlinar et al., 2005). To allow for differential anatomical origin, slices corresponding to three specific coronal sections from each animal were distributed into different experimental groups, which consisted of an equivalent number of slices from all three sections. The slices were sonicated in ice-cold 0.1 M $HClO_4$. After centrifugation, the supernatant was neutralized with phosphate buffer and analyzed

with a computer-controlled HPLC system (ESA 5006; ESA) equipped with a refrigerated autosampler and an electrochemical detector.

Statistical analysis

Statistical analysis was performed using Prism 5 (GraphPad Software). For data groups with $n < 8$, nonparametric tests were used. For data groups with $n \geq 8$, parametric tests were used if distribution was normal ($P > 0.05$) when tested with D'Agostino and Pearson omnibus normality test. Otherwise, appropriate nonparametric tests were used. Data are reported as mean ± SD, except for illustration of average time courses, where SEM is shown for clarity.

Drugs

Most of the drugs were prepared as stock solutions in distilled water. Tetrabenazine (Tbz) was prepared by dissolving Tbz free base in equimolar HCl. Concanamycin A (Folymicin) was prepared as a 10-mM stock solution in DMSO (0.05% final). All stock solutions, which were at least a thousand times the highest experimental concentration, were aliquoted and stored at $-20°C$ until use. Tbz was provided by R. Testa (Recordati S.p.A, Milan, Italy). Isoflurane was obtained from Baxter; tetrodotoxin (TTX) was from Alomone Labs; R-8-OH-DPAT, DAPV, SR-95531, and CGP-55845 were obtained from Tocris Bioscience; DNQX was from Abcam; concanamycin A, HEPES, ATP, and DMSO were from Fluka; and all other substances were obtained from Sigma-Aldrich.

RESULTS

Relative paucity of functional serotonergic synaptic transmission in the DRN

It is well recognized that, in vivo and in raphe slice preparations, the blocking of SERT-mediated 5-HT reuptake increases $[5\text{-HT}]_o$ and via activation of 5-HT1A autoreceptors suppresses serotonergic neuron firing. This indicates that there is a continuous efflux of 5-HT from
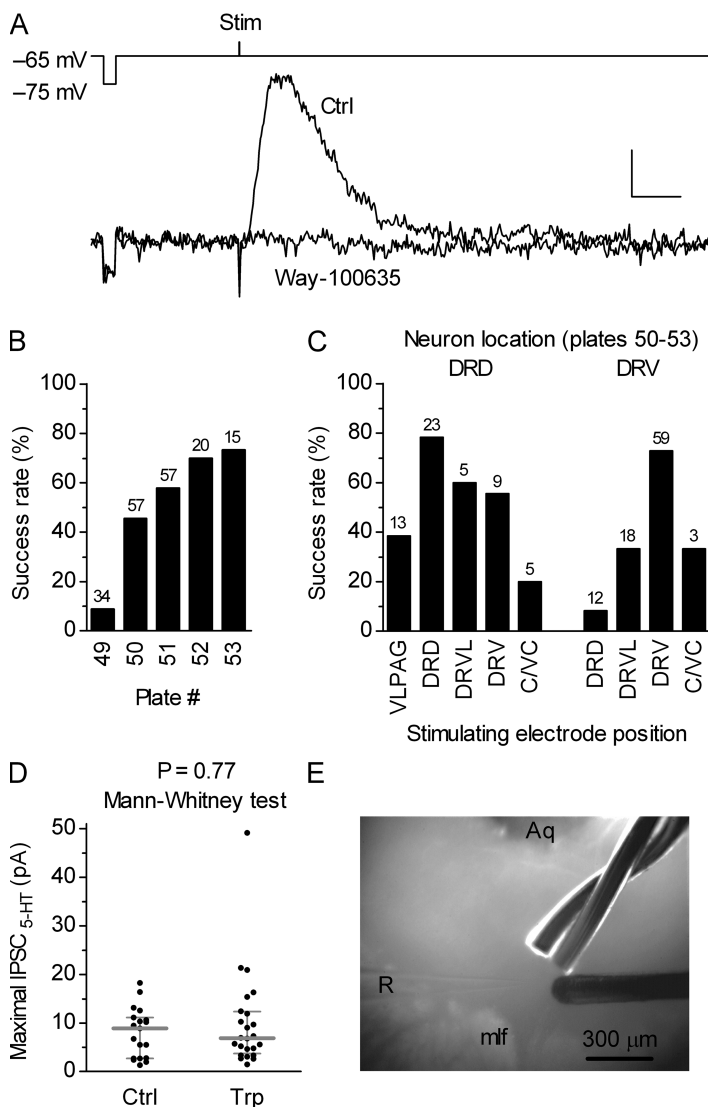

Figure 1. Relatively inconspicuous evoked IPSC$_{5\text{-HT}}$ in the DRN serotonergic neurons. (A) Electrical stimulation–evoked serotonergic postsynaptic current in a serotonergic cell is inhibited by the 5-HT1A receptor antagonist Way-100635 (50 nM). Superimposed traces are averages of 11 and 7 individual traces recorded 0–5 min before (Ctrl) and after 7–10 min of Way-100635 application. Bars, 0.5 s, 6 pA. The recording electrode voltage command and the timing of the stimulus are shown above the traces. The voltage step (10 mV) preceding the stimulus was used to monitor the input resistance (R_{IN}). The stimulus artifact is truncated. (B) Histogram summarizing percent of successfully evoked IPSC$_{5\text{-HT}}$ in the DRN serotonergic neurons with respect to the slice rostrocaudal level. Numbers of attempts are indicated above the bars. Plate numbers correspond to those of the rat brain atlas (Paxinos and Watson, 1998). (C) Histogram showing percent of successfully evoked IPSC$_{5\text{-HT}}$ in the centrocaudal part of the DRN compared with the recorded neuron location and stimulation electrode position. Numbers of attempts are indicated above the bars. DRD, dorsal raphe dorsal subnucleus; DRV, dorsal raphe ventral subnucleus; VLPAG, ventrolateral periaqueductal gray; DRVL, dorsal raphe ventrolateral subnucleus; C/VC, caudal/ventrocaudal in longitudinal slice preparation. (D) Scatter plot of the maximal IPSC$_{5\text{-HT}}$ amplitudes in a subset of experiments in which IPSC$_{5\text{-HT}}$ were evoked by using the most effective arrangement, i.e., with both the recording neuron and the stimulating electrode located in the dorsal raphe ventral subnucleus (shown in E). Comparison of responses obtained in control conditions (Ctrl; mean of 8.0 pA; median of 8.9 pA; $n = 19$; normal distribution; $P = 0.57$; D'Agostino and Pearson omnibus test) and in the presence of 5-HT precursor Trp (10 µM; mean of 10.0 pA; median of 6.9 pA; $n = 24$; nonnormal distribution; $P < 0.0001$; D'Agostino and Pearson omnibus test) revealed no significant differences between groups, indicating that the observed, relatively small maximal amplitude IPSC$_{5\text{-HT}}$ in the DRN are not caused by the reduced level of 5-HT in brain slice preparation. Symbols represent single experiments. Bars represent median with interquartile range. (E) Photograph illustrating the most effective electrode placement for evoking IPSC$_{5\text{-HT}}$ in the DRN serotonergic neurons. In 300-µm-thick slices containing the centrocaudal part of the DRN (corresponding to plates 51–53), this arrangement resulted in an ~90% success rate and the highest amplitudes of successfully evoked responses (shown in D). Two stimulating electrodes, one twisted and one concentric (right side), are positioned in the dorsal raphe ventral subnucleus ~200 µm distant form the recording electrode (R). Aq, aqueduct; mlf, medial longitudinal fasciculus.

serotonergic neurons into the surrounding extracellular space. Because serotonergic neurons display pacemaker activity during wakefulness, it is reasonable to assume that $5\text{-}HT_o$ is supplied by synaptic 5-HT release. By using whole-cell recordings in raphe neurons and electrical stimulation of nearby areas, we tested for the presence of $IPSC_{5\text{-}HT}$. In the presence of a cocktail of GABAergic and glutamatergic receptor blockers (DNQX, DAPV, SR-95531, CGP-55845, and strychnine; see Materials and methods), the electrical stimulation evoked slow inhibitory synaptic responses in serotonergic neurons. $IPSC_{5\text{-}HT}$ were nearly abolished by the selective 5-HT1A receptor antagonist Way-100635 (50 nM; 7–8 min; 95.6 ± 6.5%; mean ± SD; $n = 6$; e.g., Fig. 1 A), as expected for serotonergic synaptic responses in raphe. However, $IPSC_{5\text{-}HT}$ in the DRN were not observed in all recordings. Stimulation attempts often failed to evoke $IPSC_{5\text{-}HT}$, even with maximally attainable stimulation intensity (see Materials and methods). In total, in recordings from serotonergic neurons, $IPSC_{5\text{-}HT}$ were observed in 88 out of 191 stimulation attempts, whereas in nonserotonergic neurons, small $IPSC_{5\text{-}HT}$ (<5 pA) were observed only in 2 out of 59 cases (not depicted). A post-hoc assessment of probability of evoking an $IPSC_{5\text{-}HT}$ in serotonergic neurons revealed higher success rates in slices containing centrocaudal extent of the DRN compared with its rostral extent (Fig. 1 B). As there are no clearly delineated fiber tracts in the DRN, we tried to evoke $IPSC_{5\text{-}HT}$ by stimulating different locations in the DRN

and just outside of its dorsolateral margin. In slices containing centrocaudal extent of the DRN, the probability of evoking an $IPSC_{5\text{-}HT}$ in respect to different anatomical locations of stimulating electrodes and the recorded serotonergic neuron varied between ~8 and ~78% (Fig. 1 C). The highest success rate was obtained with both the recording neuron and the stimulated electrodes located either in the dorsal or in the ventral dorsal raphe subnucleus. A similar success rate (~70%) was previously observed by Pan et al. (1989) in slightly different conditions. Evoked $IPSC_{5\text{-}HT}$ in serotonergic neurons displayed rather small maximal amplitude. Post-hoc analysis of maximal $IPSC_{5\text{-}HT}$ amplitudes of all successful attempts in the centrocaudal extent of the DRN showed median maximal amplitude of 6.90 pA with interquartile range from 3.35 to 11.75 pA ($n = 84$; mean = 8.61 pA; nonnormal distribution; P < 0.0001; D'Agostino and Pearson omnibus test). To test for a possibility that such small responses are caused by a reduced level of 5-HT in the brain slice preparation, we compared maximal $IPSC_{5\text{-}HT}$ amplitudes in the ventral subnucleus, in which the most prominent responses were observed, in control conditions and in the presence of the 5-HT natural precursor Trp. As shown in Fig. 1 D, no significant differences were observed in the presence of 10 µM Trp compared with the control, suggesting that small maximal $IPSC_{5\text{-}HT}$ amplitude is not caused by reduced 5-HT level in brain slices. Consistent with previous structural (Descarries et al., 1982) and
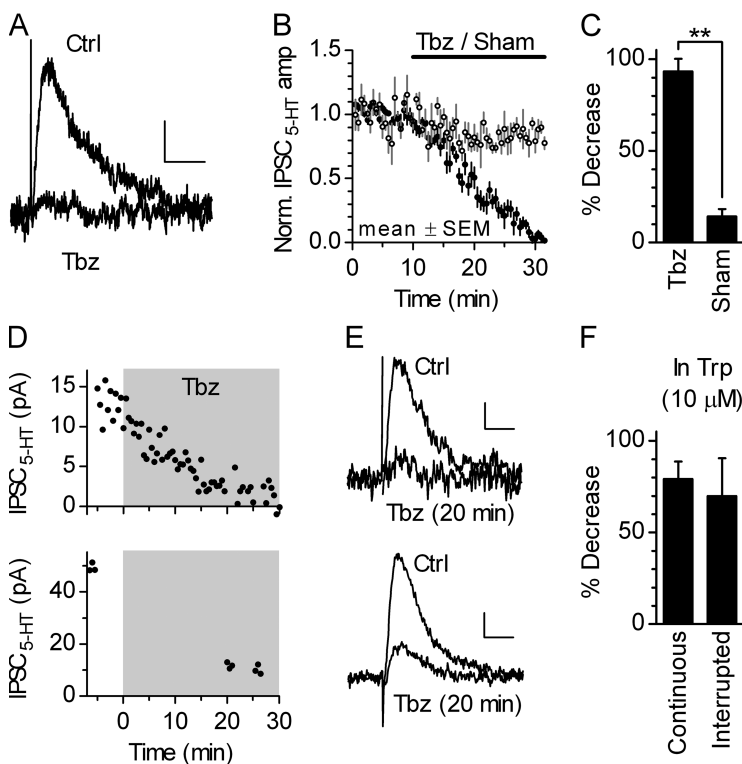

Figure 2. Inhibition of $IPSC_{5\text{-}HT}$ by the VMAT2 inhibitor Tbz. (A) Traces show evoked $IPSC_{5\text{-}HT}$ before and after 20-min application of 10 µM Tbz. Superimposed traces are averages of 21 and 11 individual traces. Bars, 1 s, 3 pA. (B) Average time course of evoked $IPSC_{5\text{-}HT}$ inhibition by 10 µM Tbz ($n = 6$; closed circles) and sham ($n = 5$; open circles). (C) Histogram summarizing the effect (mean ± SD) of 20-min-long Tbz (10 µM; $n = 6$) and sham ($n = 5$) application on evoked $IPSC_{5\text{-}HT}$ amplitude. Values for individual experiments were obtained using an average of five traces after 20–22 min of application versus average of 21 traces during the last 10 min in control. **, P = 0.0022; one-tailed Mann–Whitney test. (D and E) The effect of Tbz in the presence of 10 µM Trp with continuous and interrupted stimulation. (D) Time course of the effect of 10 µM Tbz in an experiment in which $IPSC_{5\text{-}HT}$ were evoked in a single serotonergic neuron by stimulating two separate inputs, one of which with constant stimulation (top) and the other with stimulation interrupted for the last 5 min before and the first 20 min of Tbz application (bottom). (E) Superimposed average traces of evoked $IPSC_{5\text{-}HT}$ before and after 20 min of application of Tbz of the recording shown in D. Bars, 0.5 s, 3 pA (top); 0.5 s, 10 pA (bottom). (F) Histogram summarizing the decrease in evoked $IPSC_{5\text{-}HT}$ amplitude (mean ± SD) after 20-min-long Tbz application in the presence of 10 µM Trp with continuous ($n = 5$) and interrupted ($n = 6$) stimulation. Values for individual experiments were obtained using an average of three traces. P = 0.33; one-tailed Mann–Whitney test.

functional (Pan et al., 1989) evidence, these findings indicate relative paucity of functional serotonergic synaptic transmission in the DRN.

Inhibition of IPSC$_{5-HT}$ by Tbz

In an attempt to find a pharmacological tool that can be used to assess the role of vesicular 5-HT release in the regulation of 5-HT$_o$, we wanted to verify that the depletion of vesicular 5-HT by the VMAT2 inhibitor Tbz results in IPSC$_{5-HT}$ inhibition. As shown in Fig. 2, bath perfusion of a Tbz (10 µM for 20 min), in the presence of a cocktail of GABAergic and glutamatergic receptor blockers, decreased IPSC$_{5-HT}$ by $93.4 \pm 6.9\%$ (mean ± SD; $n = 6$; Fig. 2, A–C), without changing the recording neuron R$_{IN}$ (-1.1%; SD 4.4%; P = 0.56; Wilcoxon matched pairs test) and I$_{Hold}$ (-1.5 pA; SD 6.0 pA; P = 0.84; Wilcoxon matched pairs test). We also examined dependence of the Tbz effect on 5-HT availability and the stimulation in a set of experiments in which slice

5-HT level was restored by supplementing bath solution with 10 µM Trp. To test whether Tbz-induced loss of vesicular 5-HT is facilitated by vesicle turnover caused by the stimulation, in a subset of experiments stimulation was interrupted during Tbz application. As shown in Fig. 2 (D–F), 20-min-long application of 10 µM Tbz decreased IPSC$_{5-HT}$ by $79.3 \pm 9.4\%$ (mean ± SD; $n = 5$) in the presence of continuous stimulation and by $69.9 \pm 20.8\%$ (mean ± SD; $n = 6$) in the absence of electrical stimulation. Although there was no significant differences between groups, a trend toward weaker Tbz effectiveness in conditions of interrupted stimulation suggests that stimulation-induced vesicle turnover may in some extent facilitate the effect of Tbz. Longer Tbz application in the presence of 10 µM Trp produced near-complete inhibition of IPSC$_{5-HT}$ (e.g., 28–30 min, continuous stimulation; $97.3 \pm 2.5\%$; mean ± SD; $n = 4$; not depicted), confirming the validity of Tbz as a tool to assess the role of vesicular 5-HT pool.
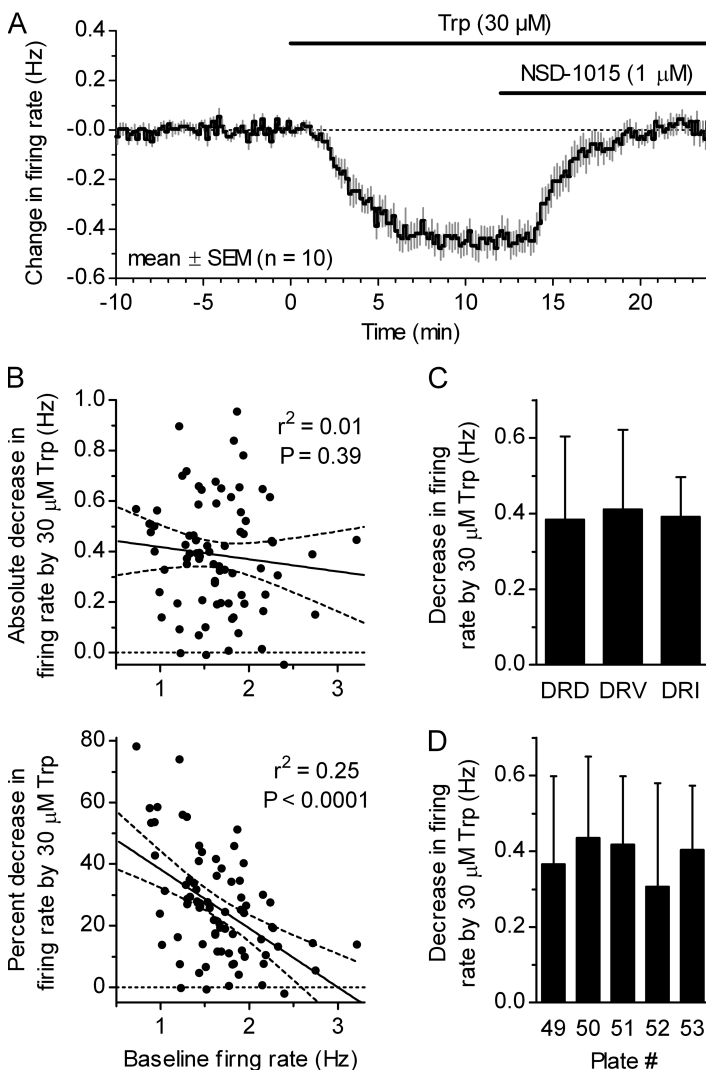

Figure 3. The characteristics of firing rate suppression by Trp. (A) Average time course of the effect of 30 µM Trp and subsequent addition of AADC inhibitor 1 µM NSD-1015 on DRN serotonergic neuron firing showing that suppression of firing by Trp depends on its conversion to 5-HT. Symbols represent the mean ± SEM of the normalized, binned firing rate. (B) The correlation between Trp effect (30 µM; 12–15 min) on serotonergic neuron firing rate expressed as absolute difference (top) or percent difference (bottom) and the baseline firing rate. Symbols represent single experiments ($n = 77$). Lines are best fits with corresponding 95% confidence intervals. r^2 and p-values refer to the linear least-square fit. (C) Histogram of the decrease in firing rate produced by 30 µM Trp in dorsal raphe subnuclei (mean, SD; $n = 46, 21$, and 3). DRD, dorsal; DRV, ventral; DRI, interfascicular subnucleus. (D) Histogram of the decrease in firing rate produced by 30 µM Trp compared with the neuron location along the rostrocaudal axis (mean, SD; $n = 13, 19, 22, 18$, and 5). Plate numbers correspond to those of the rat brain atlas (Paxinos and Watson, 1998).

Characterization of firing suppression by Trp challenge in the DRN

We wanted to investigate the origin of 5-HT$_o$ responsible for suppression of serotonergic neuron firing under physiologically relevant conditions. We previously showed that supplementing the bath solution with the 5-HT precursor Trp rescues endogenous 5-HT levels in slices and suppresses action potential firing activity via activation of 5-HT1A autoreceptors (Mlinar et al., 2005) and that, in mice, this effect of Trp is fully dependent on 5-HT1A autoreceptors and neuronal Tph2, as it is absent in slices obtained from Htr1a$^{-/-}$ (Audero et al., 2013) and Tph2$^{-/-}$ mice (Gutknecht et al., 2012). As shown in Fig. 3 A, suppression of serotonergic neuron firing by 30 µM Trp was completely reversed upon the addition of aromatic ʟ–amino acid decarboxylase (AADC) inhibitor NSD-1015 (3-hydroxybenzylhydrazine dihydrochloride), confirming that Trp conversion to 5-HT is required for firing suppression also in rat DRN (Gallager and Aghajanian, 1976; Evans et al., 2008). In control experiments, bath application of 1 µM NSD-1015 (15 min), which did not change the firing rate by itself ($-0.5 \pm 4.2\%$; mean $\pm$ SD; $n = 11$), prevented suppression of firing by subsequently added Trp (30 µM; mean = -0.7%; range from 4.0 to -3.1%; $n = 3$). In addition, firing suppression by the intermediate 5-HT precursor, 5-hydroxytryptophan (5HTP; 30 µM) was also completely reversed by 1 µM NSD-1015 (98.7 $\pm$ 3.1%; mean $\pm$ SD; $n = 5$), whereas, 30 µM 5HTP (15 min), when applied in the presence of 1 µM NSD-1015, did not change serotonergic neuron firing rate (0.1 $\pm$ 7.0%; mean $\pm$ SD; $n = 7$). Thus, experiments on raphe slices using a Trp challenge are a practical model for studying autoinhibition in in vivo–like 5-HT–synthesizing conditions. In raphe slices, the Trp challenge suppressed firing only partially, consistent with in vivo findings (Fornal et al., 1996; Hajós et al., 2001; Haddjeri et al., 2004). A post-hoc analysis of firing suppression by bath application of 30 µM Trp ($n = 77$; pooled from all experimental groups in this study) revealed that the absolute difference in firing rate before and after Trp application (-0.386 ± 0.222 Hz; mean $\pm$ SD; normal distribution; P = 0.68; D'Agostino and Pearson omnibus test) is not significantly correlated to the serotonergic neuron basal firing rate (Fig. 3 B; Spearman $r_s = -0.104$; P = 0.37), whereas when the effect of Trp is expressed as percent difference ($-25.9 \pm 17.5\%$; mean $\pm$ SD; non-normal distribution; P = 0.02; D'Agostino and Pearson omnibus test), there is a moderate correlation with the firing rate (Fig. 3 B; Spearman $r_s = -0.458$; P < 0.0001). Therefore, to eliminate the influence of the basal firing rate on the magnitude of the Trp effect, we considered the absolute difference in firing rate as the relevant parameter instead of the more commonly used fractional difference. In addition, post-hoc analysis was done to determine whether the magnitude of the Trp effect varies in respect to the recorded neuron anatomical location. We found that the Trp application suppressed firing activity similarly in the DRN subnuclei (Fig. 3 C) and along the rostro-caudal extent of the DRN (Fig. 3 D). No analysis was done in respect to the lateral axis, nor was the ventrolateral subnucleus studied, as recordings were made from neurons located mostly within 150 µm from the midline. Thus, the magnitude of firing suppression induced by bath application of 30 µM Trp exhibited a high variability but was rather uniform throughout the DRN.

Autoinhibition is independent of GABAergic and glutamatergic neurotransmission

The experiments on electrically evoked 5-HT release were performed in the presence of a cocktail of synaptic blockers and thus do not rule out the potential role of GABA and glutamate as cotransmitters or an indirect effect of the released 5-HT by modulation of neighboring GABAergic neurons and glutamatergic and GABAergic axon terminals. We therefore wanted to test whether autoinhibition depends on GABAergic and glutamatergic neurotransmission. Because local GABAergic neurons were implicated in the regulation of serotonergic neuron activity (Liu et al., 2000; Tao and Auerbach, 2003) and under basal conditions for firing rate recording, i.e., in "Trp-free" phenylephrine-supplemented ACSF, some GABAergic neurons are electrically active, we first examined whether they influence serotonergic neuron firing in slices. Under these conditions, in which autoinhibition was essentially absent, a separate or combined 15-min-long bath application of 10 µM GABAA receptor antagonist bicuculline and 3 µM GABAB receptor antagonist CGP-55845 did not significantly change the firing rate of serotonergic neurons, indicating a lack of GABAergic tone on serotonergic neurons (not depicted; bicuculline: -0.089 ± 0.181 Hz; mean $\pm$ SD; $n = 4$; P = 0.63; two-tailed Wilcoxon matched pairs test; CGP-55845: -0.023 ± 0.102 Hz; mean $\pm$ SD; $n = 6$; P = 0.84; two-tailed Wilcoxon matched pairs test; coapplication: -0.12 ± 0.18 Hz; mean $\pm$ SD; $n = 8$; normal distribution; P = 0.51; D'Agostino and Pearson omnibus test; P = 0.09; two-tailed paired t test; single unit recordings).

We next tested whether GABAergic neurotransmission influences autoinhibition in slices in which 5-HT availability was restored approximately to the physiological level by supplementing its precursor, Trp. Fig. 4 shows the effect of coapplication of GABAA receptor antagonist SR-95531 (10 µM) and GABAB antagonist CGP-55845 (3 µM) on the firing rate of serotonergic neurons, obtained by a single-unit recording in the presence of 10 µM phenylephrine and 30 µM Trp. A comparison of action potential firing rates recorded during the last minute in the antagonist mixture and during the last predrug minute revealed no significant change in the firing rate (-0.10 ± 0.14 Hz; mean $\pm$ SD;

$n = 10$; $P = 0.055$, two-tailed paired t test; normal distribution; $P = 0.19$; D'Agostino and Pearson omnibus test).

We proceeded to test the possibility that glutamatergic neurotransmission contributes to autoinhibition, as glutamate receptor–dependent 5-HT release from serotonergic cell bodies and dendrites has been demonstrated previously (De Kock et al., 2006; Colgan et al., 2012). Fig. 4 C shows the effect of coapplication of the AMPA receptor antagonist NBQX (10 µM) and the NMDA receptor antagonist DAPV (20 µM) on the firing rate of serotonergic neurons, obtained by a loose-seal cell-attached recording in the presence of 10 µM phenylephrine and 30 µM Trp. A comparison of action potential firing rates recorded during the last minute in the antagonist mixture and during the last predrug minute revealed no significant change in the firing rate

$(-0.048 \pm 0.080$ Hz; mean $\pm$ SD; $n = 8$; $P = 0.141$; two-tailed Wilcoxon matched pairs test; nonnormal distribution; $P = 0.005$; D'Agostino and Pearson omnibus test). These experiments showed that GABAergic and glutamatergic transmission do not contribute significantly to serotonergic neuron autoinhibition when in vivo–like 5-HT–synthesizing conditions were restored by Trp supplementation.

Autoinhibition is mediated by nonvesicular 5-HT release

Because both cytoplasmic and vesicular release of 5-HT have been implicated in the regulation of 5-HT_o, we investigated their respective involvement in serotonergic neuron autoinhibition. The role of vesicular 5-HT pool was assayed with the VMAT2 inhibitor Tbz. When tested under basal conditions characterized by virtually absent autoinhibition, i.e., in phenylephrine-supplemented
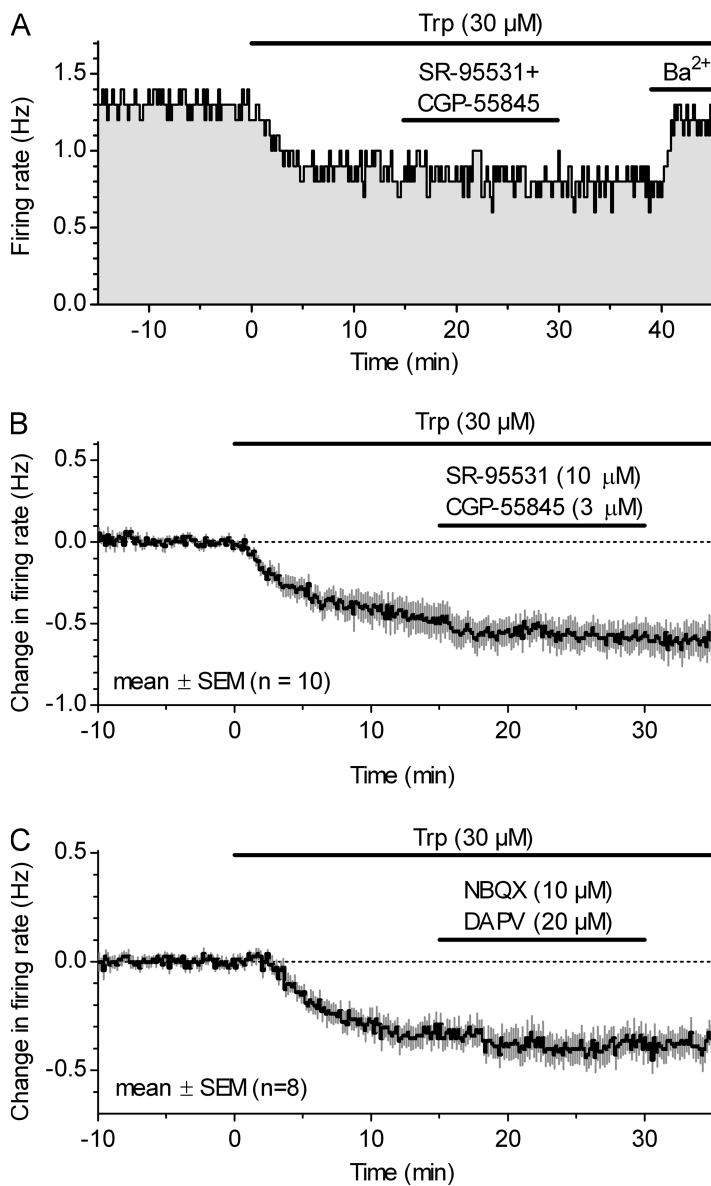

Figure 4. Autoinhibition is independent of GABAergic and glutamatergic transmission. Suppression of the serotonergic neuron firing rate by Trp is not influenced by GABA and glutamate receptor block in single-unit (A and B) and loose-seal cell-attached (C) recordings in phenylephrine-supplemented ACSF. (A) Time course of a representative experiment with coapplication of GABAA (SR-95531; 10 µM) and GABAB (CGP-55845; 3 µM) receptor antagonists. At the end of the recording, Trp-induced suppression of firing was reversed by the application of GIRK channel blocker Ba^{2+} ($BaCl_2$; 150 µM). (B) Summary time course of experiments showing that coapplication of 10 µM SR-95531 and 3 µM CGP-55845 did not change the firing rate in the presence of 10 µM phenylephrine and 30 µM Trp. Symbols represent the mean of the normalized, binned firing rate, expressed as absolute difference in the baseline firing rate computed over the 5-min preceding Trp application in each experiment. (C) Summary time course of experiments showing lack of effect of coapplication of AMPA and NMDA receptor antagonists on the firing rate. Symbols represent the mean of the normalized, binned firing rate.

ACSF, the application of 10 µM Tbz slightly but significantly reduced DRN serotonergic neuron firing rate (Fig. 5, A and B) and partially depleted 5-HT content in slices from the predrug level of 1.93 ± 0.84 pmol mg^{-1} to 1.21 ± 0.44 pmol mg^{-1} in 10 min, and to 1.02 ± 0.45 pmol mg^{-1} in 25 min, respectively (mean ± SD; $n = 9$; Fig. 5 C). The effect of Tbz on firing was reversible upon the addition of the 5-HT1A receptor antagonist Way-100635 (50–100 nM; $n = 5$; not depicted; e.g., Fig. 5 A) or GIRK channel blocker Ba^{2+} (BaCl$_2$; 150 µM; $n = 6$; not depicted). These effects of Tbz are consistent with its vesicle-depleting action, which occurred over the same time interval as the decrease in IPSC$_{5-HT}$ (20–25 min; Fig. 2) and as reported previously for a voltammetry-detected decrease in the electrical stimulation–evoked 5-HT release (Bunin et al., 1998). The small reduction in neuron firing rate by Tbz in spite of the decrease in overall slice 5-HT content is likely attributable to leakage of vesicular 5-HT to cytosol and the consequent shift in equilibrium between cytosolic and extracellular 5-HT levels, which then resulted in an increased [5-HT]$_o$ (Fig. 5 D).

We next wanted to test whether depletion of vesicular 5-HT reverses Trp-induced autoinhibition, an effect that would occur if serotonergic neuron firing is under autoinhibitory control by exocytotic 5-HT release. For this, we examined the effect of 10 µM Tbz (15 min) on the firing rate in the presence of 10 µM phenylephrine and 30 µM Trp (Fig. 6, A and B). A comparison of firing rates during the last 3 min before Tbz (1.446 ± 0.367 Hz; mean ± SD; $n = 15$; normal distribution; P = 0.06; D'Agostino and Pearson omnibus test) and during the last 3 min of Tbz application (1.300 ± 0.537 Hz; mean ± SD; $n = 15$; normal distribution; P = 0.15; D'Agostino and Pearson omnibus test) revealed no significant change in firing rate, although a reducing trend was observed (−0.146 ± 0.282 Hz; $n = 15$; P = 0.058; two-tailed Wilcoxon matched pairs test; nonnormal distribution; P = 0.0046; D'Agostino and Pearson omnibus test). We also confirmed that 30 µM Trp suppressed firing when
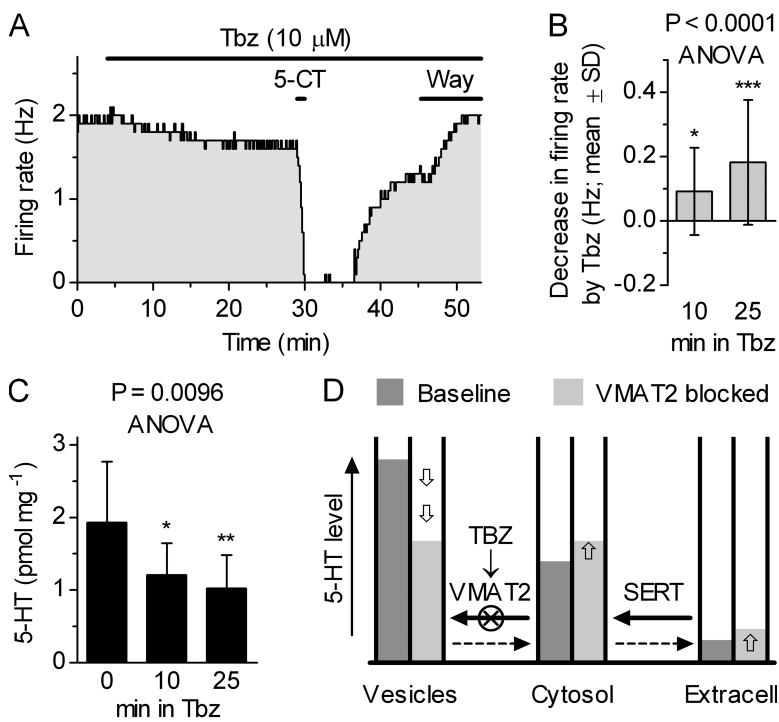

Figure 5. Effects of VMAT2 inhibitor Tbz in raphe slices. (A) Time course of a representative experiment in phenylephrine-supplemented ACSF, showing the decrease in firing rate produced by 10 µM Tbz. The neuron was confirmed serotonergic, as its firing was abolished in response to bath perfusion of the 5-HT1A receptor agonist 5-CT (10 nM). The application of 50 nM Way-100635 (Way) restored the firing rate to the level preceding Tbz, indicating that the effect of Tbz was mediated by 5-HT1A autoreceptors. (B) Histogram summarizing the effect of 10 µM Tbz on firing in phenylephrine-supplemented ACSF. Firing rates recorded at 9–10 and 22–25 min of the Tbz application were compared with the firing rate recorded during the last 5 min in control. Repeated measures one-way ANOVA revealed a significant decrease in the firing rate by Tbz ($n = 19$; P < 0.0001; normal distribution; P = 0.23, 0.08, and 0.09; D'Agostino and Pearson omnibus test). After 10 min of Tbz application, the firing rate was decreased by 0.092 ± 0.136 Hz (mean ± SD; *, P < 0.05; Dunnett's post-hoc test vs. the baseline), whereas at 25 min, the firing rate was decreased by 0.182 ± 0.194 Hz (mean ± SD; ***, P < 0.001; Dunnett's post-hoc test vs. the baseline). (C) Histogram summarizing the effect of 10 µM Tbz on 5-HT content (pmol mg^{-1} wet tissue) in raphe slices. Columns represent average values for nine slices obtained from nine animals. Error bars denote SD. The left column represents control slices, perfused for 30 min in the experimental chamber with ACSF containing 3 µM phenylephrine at 34°C. The middle and right columns represent slices that were additionally perfused with ACSF containing 3 µM phenylephrine and 10 µM Tbz for 10 and 25 min, respectively. The groups were significantly different (P = 0.0096; two-tail one-way ANOVA; normal distribution; P = 0.05, 0.29, and 0.97; D'Agostino and Pearson omnibus test; *, P < 0.05; **, P < 0.01; Dunnett's post-hoc test vs. control). (D) Schematic diagram illustrating the expected redistribution of 5-HT after Tbz application. Concentration gradients of 5-HT across vesicular (>10^4-fold; Schuldiner et al., 1995) and plasma membrane (≥10^3-fold; Adams and DeFelice, 2002) are generated and maintained by VMAT2 and SERT, respectively. Block of VMAT by Tbz slowly dissipates the 5-HT gradient across the vesicular membrane, resulting in a decrease in vesicular 5-HT concentration and an increase in cytosolic 5-HT concentration, which in turn leads to an increase in [5-HT]$_o$ via reequilibration of plasma membrane 5-HT gradient. Dashed arrows indicate flux of 5-HT down the gradient and open arrows indicate direction of changes in 5-HT concentration within each compartment. Degradation of excessive cytosolic 5-HT by MAOB (K$_m$ of ≈1.2 mM; Fowler and Tipton, 1982) limits the increase in 5-HT concentration, resulting only in a weak reduction in the firing rate.

applied 30–45 min after Tbz (Fig. 6, C and D). Finally, we asked whether these experiments with Tbz could be reproduced with a chemically unrelated substance that depletes secretory vesicles through a different mechanism. For this purpose, we used the specific inhibitor of vacuolar-type H^+-ATPase (V-ATPase), concanamycin A (Fig. 6, E and F). A comparison of firing rates during the last 3 min before concanamycin A (1.456 ± 0.561 Hz; mean ± SD; $n = 9$; normal distribution; P = 0.90; D'Agostino and Pearson omnibus test) and during the last 3 min of the application (1.465 ± 0.572 Hz; mean

± SD; $n = 9$; normal distribution; P = 0.96; D'Agostino and Pearson omnibus test) revealed no significantly change in the firing rate by concanamycin A (0.009 ± 0.087 Hz; $n = 9$; P = 0.76; two-tailed paired t test). Collectively, these experiments indicated that autoinhibition of the DRN serotonergic neuron firing is mediated by nonvesicular 5-HT release.

Autoinhibition is not mediated by SERT reverse transport

The physiological function of SERT is the reuptake of 5-HT_o, but SERT can operate in reverse direction, which
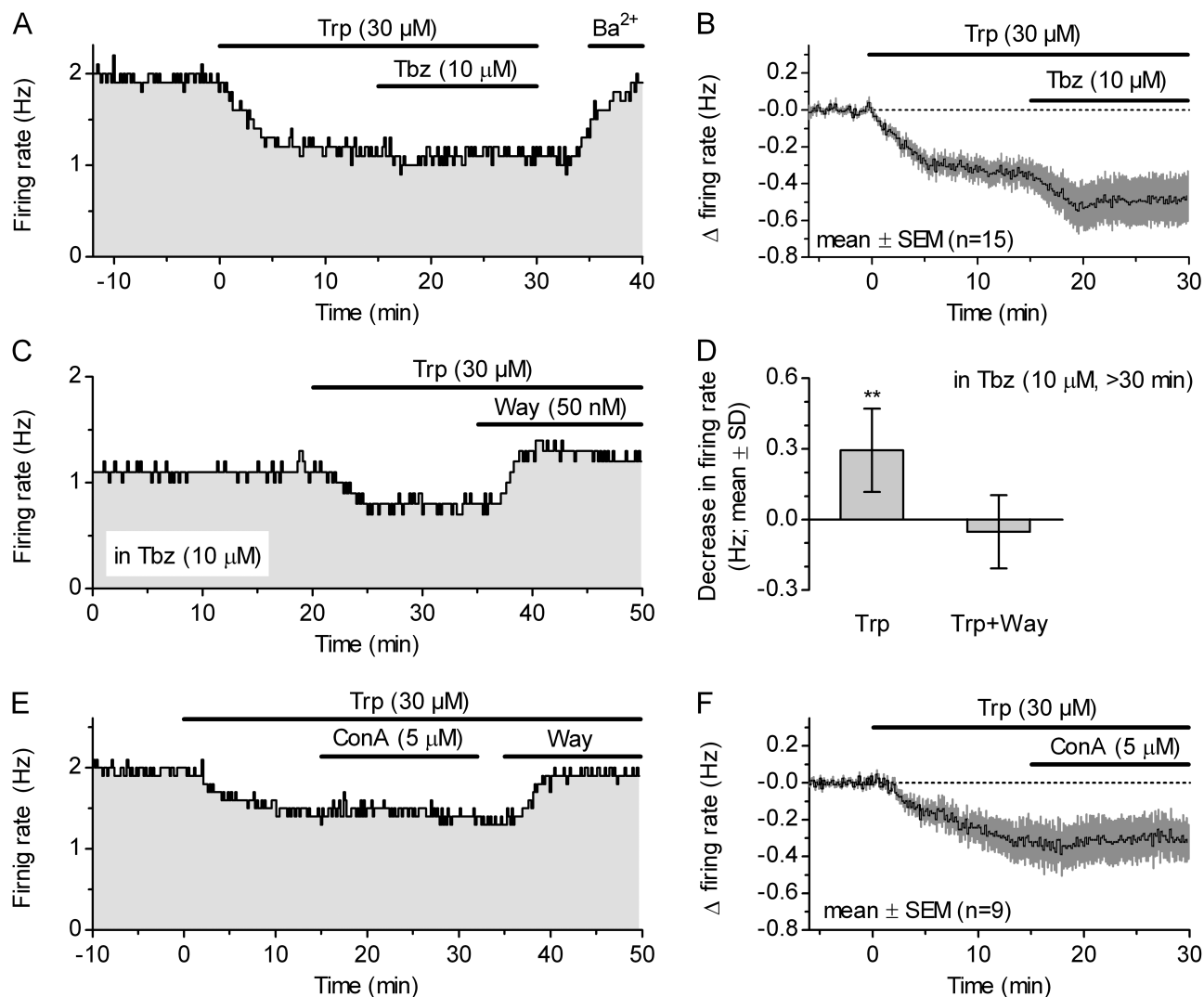

Figure 6. Autoinhibition is not mediated by vesicular release of 5-HT. (A) Time course of a representative recording showing that suppression of the firing rate by 30 µM Trp was not affected by subsequent addition of 10 µM Tbz, whereas it was reversed by the addition of 150 µM $BaCl_2$ (Ba^{2+}). (B) Average time course of the effect of 30 µM Trp and subsequent addition of 10 µM Tbz on DRN serotonergic neuron firing. Symbols represent the mean ± SEM of the normalized, binned firing rate. (C) Time course of a representative recording illustrating suppression of the firing rate by 30 µM Trp in the presence of 10 µM Tbz. The effect of Trp was reversed by the addition of Way-100635. (D) Histogram summarizing the effect of 30 µM Trp in the presence of Tbz and the cocktail of glutamatergic and GABAergic blockers. After 15 min of Trp application, the firing rate was decreased by 0.295 ± 0.177 Hz (mean ± SD; $n = 8$; **, P = 0.0011; one-tailed paired t test; normal distribution; P = 0.41; D'Agostino and Pearson omnibus test). (E) Time course of a representative recording showing that suppression of the firing rate by 30 µM Trp was not affected by subsequent addition of the V-ATPase inhibitor concanamycin A (ConA; 5 µM), whereas it was reversed by the addition of 100 nM Way-100635. (F) Average time course of the effect of 30 µM Trp and the subsequent addition of 5 µM concanamycin A. Symbols represent the mean ± SEM of the normalized, binned firing rate.

results in a net efflux of cytosolic 5-HT. Having established that 5-HT release underlying autoinhibition is nonvesicular and hence from the cytoplasmic pool, we wanted to test the possibility that reverse transport of 5-HT via SERT contributes to autoinhibition. The effect of SERT inhibition on the firing rate was studied by the application of citalopram, an SSRI that blocks SERT without inducing 5-HT efflux (Sitte et al., 2000). As shown in Fig. 7 (A and B), the dose–response relationship of citalopram showed properties consistent with the single effect of inhibiting 5-HT reuptake. Under basal conditions ("Trp-free" ACSF), inhibition of SERT by citalopram decreased the firing rate with an EC_{50} of 73.7 nM (41.3–131.7 nM; 95% confidence interval [C.I.]) and caused a near-complete suppression of firing (fit bottom = 2.1%; −18.8 to 23.0%; 95% C.I.), revealing substantial continuous efflux of 5-HT, even in slices having reduced 5-HT content (∼60%; Mlinar et al., 2005). Under conditions where vesicular 5-HT accumulation was inhibited by Tbz, citalopram was similarly effective (EC_{50} = 94.5 nM; 46.0–194.3 nM; 95% C.I.; log IC_{50} not different from Ctrl, P = 0.58, F = 0.32, extra sum-of-squares F test), although a clear trend toward

weaker maximal effect was observed (fit bottom = 26.7%; 9.7–43.6%; 95% C.I.; not different from Crtl, P = 0.10, F = 2.71, extra sum-of-squares F test). Importantly, at the highest concentrations of citalopram applied, 1–3 µM, expected to completely inhibit SERT, firing was maximally suppressed, indicating that SERT reversal does not contribute to the release. On the other hand, an apparently weaker potency of citalopram in the presence of Tbz defies easy explanation. It could be a consequence of redistribution of endogenous 5-HT after VMAT2 inhibition, in particular to the additional decrease in 5-HT content (see Fig. 5, C and D), as well as a direct consequence of decreased vesicular 5-HT release. To distinguish between these possibilities, the effect of SERT inhibition on firing was also studied in a higher number of neurons, under conditions of different levels of cytosolic and vesicular 5-HT. We compared the effects of partial inhibition of SERT by 30 nM citalopram (25 min) in baseline conditions (Trp-free ACSF), and in the continuous presence of Tbz or Trp, as well as coapplied Tbz and Trp (Fig. 7 C). To obtain matching precitalopram firing rates among experimental groups, Trp was used at 10 µM, the concentration that
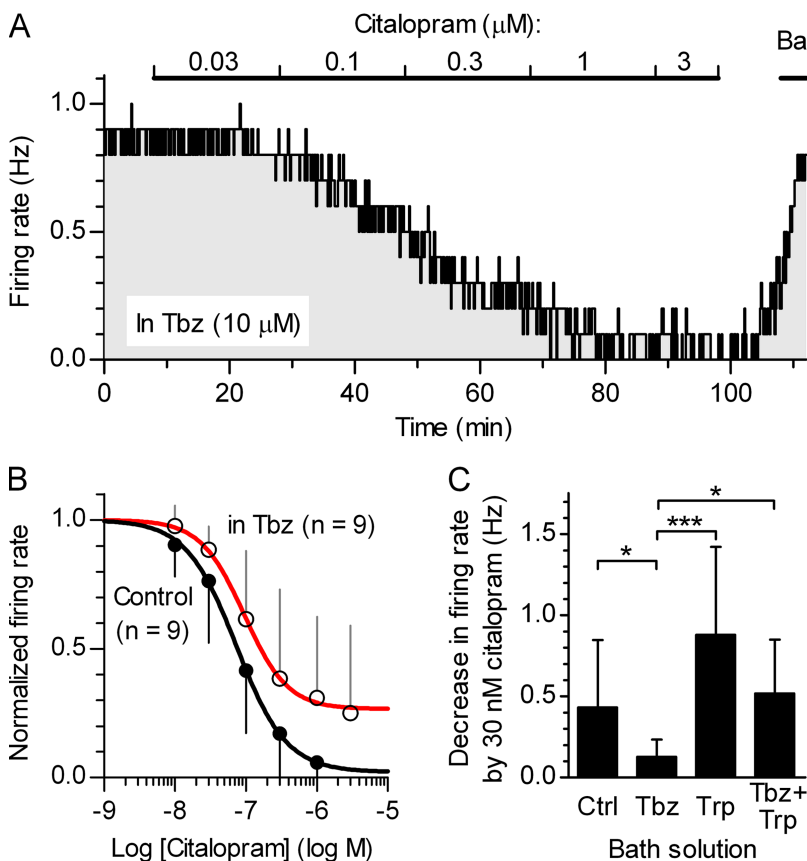

Figure 7. 5-HT release is not mediated by SERT reversal. (A) A representative recording showing the response of a DRN serotonergic neuron to increasing citalopram concentrations in the continuous presence of 10 µM Tbz. Ba, 150 µM $BaCl_2$. (B) Comparison of concentration–response relationships for citalopram obtained in the presence of 10 µM Tbz and in control conditions. Individual points correspond to arithmetic means of firing rate normalized to the baseline firing rate; error bars represent SD. Solid lines are the best least-squares fit to the logistic equation, $b + (1 − b)/(1 + (EC_{50}/[Citalopram])^{n_H})$, where EC_{50} is the half-maximally effective concentration, n_H is the Hill coefficient, and b is the fraction remaining at the maximal citalopram effect (R^2 = 0.72, control; 0.47 in Tbz). (C) Histogram summarizing change in action potential firing rate by partial inhibition of SERT by 30 nM citalopram (25th min vs. last 5 min before citalopram) in control (Ctrl, n = 24), Tbz (10 µM for 20 min; n = 14), Trp (10 µM for 30 min; n = 12), and Tbz plus Trp (10 µM each for 30 min; n = 8). Error bars represent SD. The firing was significantly reduced by 30 nM citalopram in all conditions (P < 0.0001, Ctrl; P = 0.0006, Tbz; P = 0.0005, Trp; P = 0.008, Tbz + Trp; Wilcoxon matched pair test). The effect of citalopram was significantly different among the groups (P = 0.0002, Kruskal–Wallis test; Ctrl: nonnormal distribution, P = 0.001; Tbz: normal distribution, P = 0.70; Trp: normal distribution, P = 0.27; Tbz + Trp: nonnormal distribution, P = 0.008; D'Agostino and Pearson omnibus test). Dunn's post-hoc test revealed statistically significant differences for the citalopram effect between the Tbz and control groups (P < 0.05), between the Tbz and Trp groups (P < 0.001), and between the Tbz and Tbz + Trp groups (P < 0.05).

suppresses firing to an extent comparable with that to 10 µM Tbz, while partially rescuing slice 5-HT content (Mlinar et al., 2005). Similar to the concentration–response experiments, partial inhibition of SERT by citalopram suppressed firing less in the Tbz group than in the control group. However, under conditions where the bath solution contained 10 µM Trp, regardless of the presence of Tbz, the effect of citalopram was restored to near-control level (trend toward stronger effect in Trp group) and was significantly stronger compared with the Tbz group (P = 0.0002; Kruskal–Wallis test; see Fig. 7 C legend). These findings support the hypothesis that the citalopram effect depends on cytosolic 5-HT levels and suggest that VMAT2-dependent vesicular 5-HT accumulation is not required for continuous 5-HT release unmasked upon the partial inhibition of SERT-mediated reuptake by citalopram.

Autoinhibition persists in the absence of neuronal firing
We next wanted to examine the dependence of autoinhibition and the underlying 5-HT efflux on serotonergic neuron firing, a question difficult to answer by using their firing rate as the monitored parameter. Given that the activation of 5-HT1A autoreceptors suppresses the firing of DRN serotonergic neurons primarily by activation of GIRK channels, to examine whether firing activity is required for 5-HT release, we investigated the effects of perturbation of endogenous 5-HT on 5-HT1A autoreceptor-activated GIRK current in the presence of TTX in whole-cell configuration. Because the optimal conditions for whole-cell recording of GIRK current are different from those for the firing rate recording (thinner slices, younger animals, lower temperature, higher $[K^+]_o$, and the absence of phenylephrine), we first tested whether 5-HT precursors, Trp and 5HTP, and the SSRI citalopram produce a measurable increase in GIRK conductance. In preliminary experiments performed in the synaptic blocker cocktail (e.g., Fig. 8, A and B), substances that suppressed firing in cell-attached recordings produced an increase in GIRK conductance, which was reversed by the 5-HT1A receptor antagonist Way-100635, indicating that 5-HT1A autoreceptor-activated GIRK channels can be used as a 5-HT_o sensor. Because the effect of 30 µM Trp was at the threshold of detectability in these recordings (0.25 ± 0.08 nS; mean ± SD; n = 4), possibly because of reduced Tph2 activity, whereas 30 µM 5HTP and 0.2–1 µM citalopram consistently increased GIRK conductance (see Fig. 8 H, open bars), we also used the 5HTP challenge to elevate endogenous 5-HT in whole-cell experiments, in addition to the Trp challenge.

We proceeded to investigate whether 5-HT release in the DRN depends on neural activity. Under conditions where neuronal firing activity was abolished by bath application of 0.5 µM TTX, the application of 30 µM 5HTP (n = 3) or 1 µM citalopram (n = 3) produced an increase in inwardly rectifying K^+ conductance that was reversed by the addition of 50 nM Way-100635 (Fig. 8, C–E; representative of three experiments), indicating the persistence of 5-HT efflux in the absence of firing. A similar increase in GIRK conductance by 1 µM citalopram (n = 3) was also obtained in conditions where both vesicular accumulation of 5-HT and action potential firing activity were prevented by bath application of 10 µM Tbz (in bath solution for at least 25 min before the start of the experiment) and TTX. As shown in Fig. 8 (F and G), the addition of 30 µM Trp in the presence of TTX, Tbz, and citalopram produced an increase in GIRK conductance (mean 2.5 nS; range of 2.2 to 2.7 nS; n = 3; corresponding to an estimated increase in $[5\text{-HT}]_o$ of ≈80 nM; see Materials and methods), indicating that autoinhibition and the underlying 5-HT efflux persist under conditions where firing activity, vesicular 5-HT release, and SERT-mediated reuptake are abolished. Under these conditions, the time course of Trp-induced increase in GIRK conductance reflects the time course of cytosolic 5-HT efflux across the plasma membrane. The rate of GIRK conductance increase upon Trp application corresponds to the lower limit of 5-HT release because the Trp-induced increase in GIRK conductance is a multistep process. In three recordings, data could be well fitted with a single-exponential association function (R^2 = 0.92–0.98; see Fig. 8 legend), revealing that after a lag of 2–3 min upon the application of Trp, GIRK conductance increased at a mean time constant of 86.6 s (range of 82.3 to 89.0 s), indicating that 5-HT release occurs at least at the same rate. Similar results were obtained under control conditions, i.e., in the cocktail of synaptic blockers (τ = 128.5 s; range of 89.7 to 193.5 s; n = 3; e.g., Fig. 8 A). As summarized in Fig. 8 H, by using 5-HT1A autoreceptor-activated GIRK conductance as a 5-HT_o sensor, we show that firing activity is not required for autoinhibition and that substantial continuous efflux of cytosolic 5-HT occurs in DRN.

Extracellular Ca^{2+} and voltage-gated Ca^{2+} channels (VGCCs) are not required for 5-HT efflux
Because extracellular Ca^{2+} is required for exocitotic neurotransmitter release, we wanted to examine dependence of 5-HT efflux in the DRN on extracellular Ca^{2+}. Preliminary experiments showed that prolonged whole-cell recordings from serotonergic neurons in Ca^{2+}-free extracellular solution are not feasible as a result of of gradual developing of ohmic leak starting 20–30 min after establishing of whole-cell recording configuration. Therefore, to test whether 5-HT efflux can activate GIRK conductance in the absence of extracellular Ca^{2+}, we applied briefer experimental protocols in which slices were perfused for at least 30 min before the start of the recording, with bath solution containing zero Ca^{2+} (substituted with Mg^{2+}); 5.5 mM K^+; and the cocktail
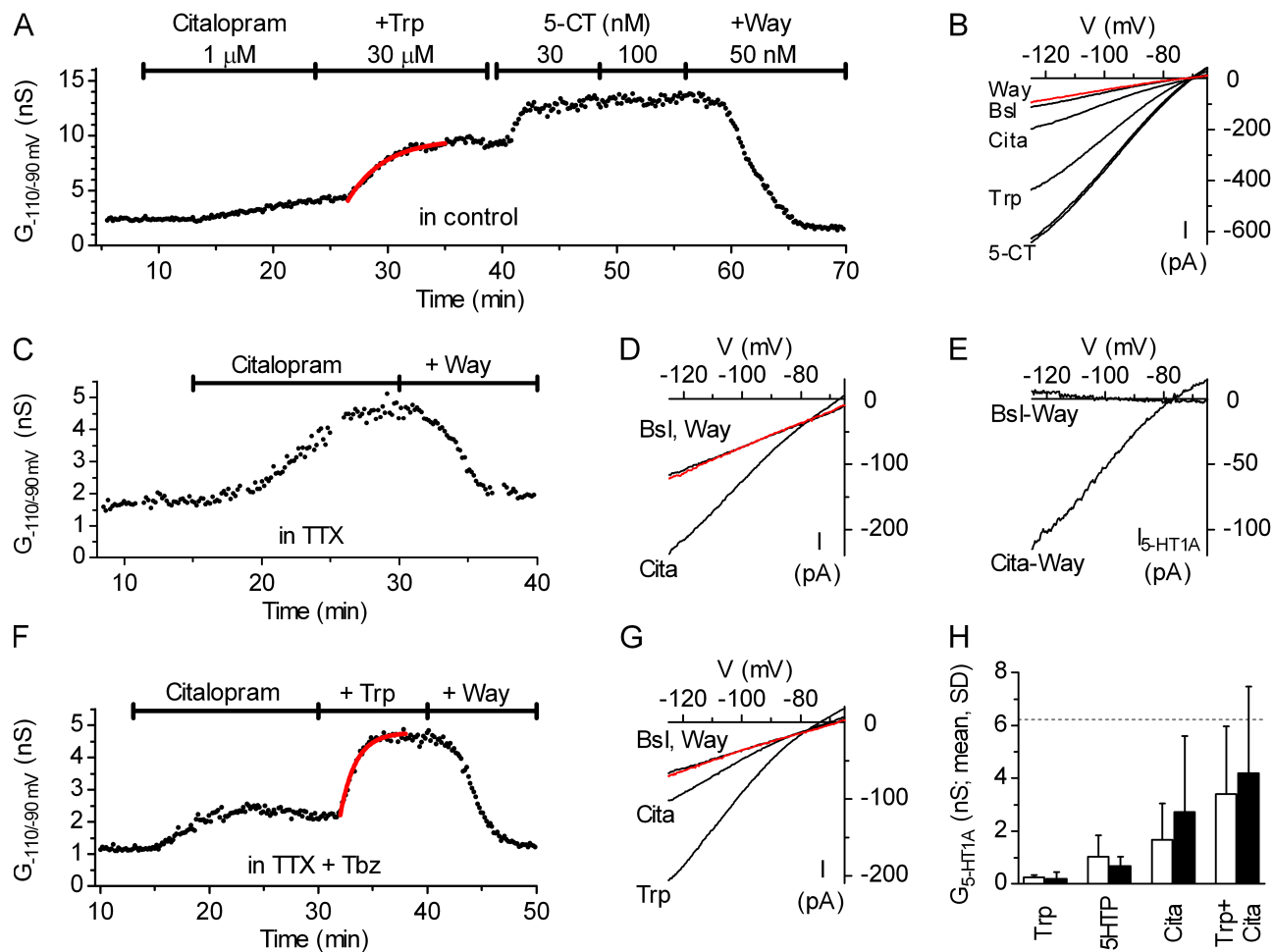
Figure 8. Use of 5-HT1A autoreceptor-activated GIRK channels of patched neuron as 5-HT$_o$ sensor reveals that firing activity is not required for autoinhibition. (A) Time course of a representative experiment under control conditions (cocktail of synaptic blockers, 5.5 mM [K$^+$]$_o$; see Materials and methods) illustrating the effect of citalopram, coapplication of citalopram and Trp (+Trp), and 5-CT and the subsequent addition of Way-100635 (+Way) on inwardly rectifying K$^+$ conductance (G$_{-110/-90mV}$). 5-CT and Way-100635 were applied to determine maximal and zero 5-HT1A autoreceptor-activated GIRK conductance (G$_{5-HT1A}$), respectively. In this and in subsequent figures showing time courses of whole-cell experiments, the sign + denotes the application of the compound in the continuous presence of preceding compounds, whereas time indicates duration of whole-cell configuration. The red curve is the data fit (from 26.5 to 35 min) with the function of the form G = G$_{cita}$ + (G$_{Trp}$ − G$_{cita}$)(1 − e$^{t/\tau}$), where G is conductance and τ is the exponential time constant (τ = 193.5 s; 171–223 s 95% C.I.; R^2 = 0.982). (B) The current–voltage plot shows inwardly rectifying K$^+$ currents of the same experiment recorded before citalopram application (Bsl), in citalopram (Cita), after the addition of Trp, in 30 and 100 nM 5-CT, and after the addition of Way-100635 (Way; red trace). Traces are averages of the last 12 individual ramps recorded under the indicated conditions. (C) Time course of a representative experiment illustrating the effect of 1 µM citalopram and its antagonism after the addition of 50 nM Way-100635 (+Way) in the presence of 0.5 µM TTX. TTX was applied 3 min after establishing whole-cell configuration after identification of the neuron as serotonergic based on its properties in current clamp. Na$^+$ channel block by TTX was facilitated and verified by periodic current injections that evoked action potential firing. (D) Current–voltage plot of the same experiment. Traces are averages of the last 12 individual ramps recorded before (Bsl) and during citalopram application (Cita), and the last six ramps recorded after the addition of Way-100635 (Way; red trace). (E) Current–voltage plot of net 5-HT1A autoreceptor-activated GIRK current (I$_{5-HT1A}$) obtained by subtraction of Way-100635–insensitive current shows essentially no I$_{5-HT1A}$ under baseline conditions and prominent activation in the presence of citalopram. (F) Time course of a representative experiment illustrating the effect of 1 µM citalopram and the subsequent addition of 30 µM Trp (+Trp) and 50 nM Way-100635 (+Way) in the presence of 0.5 µM TTX and 10 µM Tbz. The red curve is the data fit (from 32 to 38 min) with the function described in A (τ = 85.2 s; 77.1–95.2 s 95% C.I.; R^2 = 0.978). (G) Current–voltage plot of the same experiment. Traces are averages of 12 individual ramps, except for that in Way (six ramps; red trace). (H) Histogram summarizing 5-HT1A autoreceptor-mediated activation of GIRK conductance by 30 µM Trp, 30 µM 5HTP, and 1 µM citalopram (Cita), and coapplication of 30 µM Trp and 1 µM citalopram (Trp + Cita) in the synaptic blocker cocktail (open bars; n = 4, 4, 8, and 6) and in the presence of TTX or TTX and Tbz (pooled data, closed bars; n = 6, 3, 6, and 6). In individual experiments, G$_{5-HT1A}$ values for the substances applied were obtained by subtracting the mean of G$_{-110/-90mV}$ values measured in baseline and in 50 nM Way-100635. The dotted line indicates the mean maximal G$_{5-HT1A}$, determined by use of 30 nM 5-CT (see Materials and methods).

of synaptic blockers, 0.5 µM TTX, 10 µM Trp, and 10 µM Tbz. Under these conditions, block of 5-HT uptake by bath application of 1 µM citalopram during the recording (15–18 min; $n = 6$; Fig. 9, A and B) or before the establishment of whole-cell recording configuration (25–30 min; $n = 3$; Fig. 9 C) produced a clear activation of 5-HT$_{1A}$ receptor-activated GIRK conductance, as revealed by the subsequent addition of 20 nM Way-100635 (10–12 min; Fig. 9 D). Because Ca^{2+}-free extracellular solution used in these experiments contains low micromolar Ca^{2+} (contamination from MgCl$_2$ and glassware), we also examined whether VGCCs are required for 5-HT efflux. As shown in Fig. 9 (E–H), in recordings with bath solution containing 100 µM of nonselective VGCC blocker Cd^{2+} (CdCl$_2$), 5.5 mM K$^+$, and the cocktail of synaptic blockers (0.5 µM TTX, 10 µM Trp, and 10 µM Tbz), the application of 1 µM citalopram activated GIRK conductance to an extent similar to that observed in Ca^{2+}-free solution. Thus, 5-HT release persisted under conditions where, in addition to abolished firing activity and vesicular 5-HT accumulation, extracellular solution was devoid of Ca^{2+} or contained Cd^{2+}, preventing Ca^{2+} entry through VGCCs. Collectively, these findings further strengthened the conclusion that substantial nonexocitotic 5-HT efflux occurs in the DRN.

5-HT efflux from a neuron does not significantly contribute to its own autoinhibition

We next investigated the origin of 5-HT underlying autoinhibition in the DRN. To examine a possible contribution of 5-HT efflux from an individual serotonergic neuron to autoinhibition, we performed a series of experiments in which inwardly rectifying K$^+$ conductance was measured under conditions where 5-HT or its intermediate precursor, 5HTP, was included in the pipette solution (Fig. 10). Because the exact concentration
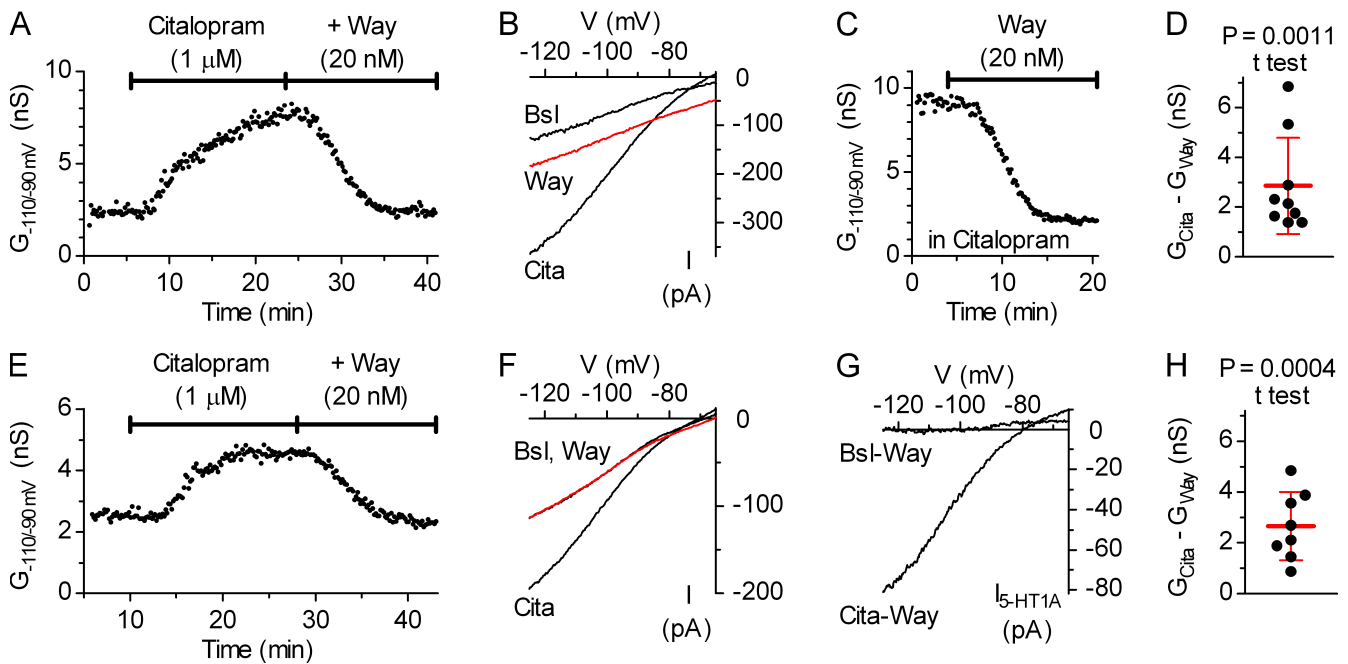

Figure 9. Extracellular Ca^{2+} is not required for autoinhibition. (A–D) Experiments in Ca^{2+}-free extracellular solution. (A) Time course of a representative experiment ($n = 6$) illustrating the effect of 1 µM citalopram and its antagonism after the addition of 20 nM Way-100635 (+Way) in Ca^{2+}-free extracellular solution, containing the cocktail of synaptic blockers: 5.5 mM [K$^+$]$_o$, 0.5 µM TTX, 10 µM Tbz, and 10 µM Trp. (B) The current–voltage plot of the same experiment. Traces are averages of the last nine individual ramps recorded before citalopram application (Bsl), in citalopram (Cita), and after the addition of Way-100635 (Way; red trace). Downward shift of the trace in Way in respect to the Bsl was caused by the gradual increase in leak, typical for recordings in Ca^{2+}-free extracellular solution. (C) Time course of a representative experiment ($n = 3$) in which 1 µM citalopram was applied 30 min before obtaining whole-cell recording configuration, permitting the completion of the experiment under leak-free conditions. (D) Scatter plot summarizing the magnitude of 5-HT$_{1A}$ autoreceptor-mediated activation of GIRK conductance by 1 µM citalopram in Ca^{2+}-free extracellular solution. Error bars correspond to mean ± SD. The addition of Way-100635 in the continuous presence of citalopram decreased inwardly rectifying K$^+$ conductance by 2.86 ± 1.93 nS (mean ± SD; $n = 9$; P = 0.0011; one-tailed paired t test; normal distribution; P = 0.07; D'Agostino and Pearson omnibus test). (E–H) Experiments in the presence of the nonselective VGCC blocker Cd^{2+}. (E) Time course of a representative experiment in extracellular solution containing the cocktail of synaptic blockers: 5.5 mM [K$^+$]$_o$, 0.5 µM TTX, 10 µM Tbz, 10 µM Trp, and 100 µM CdCl$_2$. (F) The current–voltage plot of the same experiment. Traces are averages of 13 individual ramps recorded under the indicated conditions. (G) Current–voltage plot of net 5-HT1A autoreceptor-activated GIRK current (I$_{5-HT1A}$) of the same experiment. The trace in Way-100635 is shown in red. (H) Scatter plot summarizing the magnitude of 5-HT$_{1A}$ autoreceptor-mediated activation of GIRK conductance by 1 µM citalopram in Cd^{2+}-containing extracellular solution. Bars correspond to mean ± SD. The addition of 20 µM Way-100635 decreased inwardly rectifying K$^+$ conductance by 2.66 ± 1.35 nS (mean ± SD; $n = 8$; P = 0.0004; one-tailed paired t test; normal distribution; P = 0.77; D'Agostino and Pearson omnibus test).
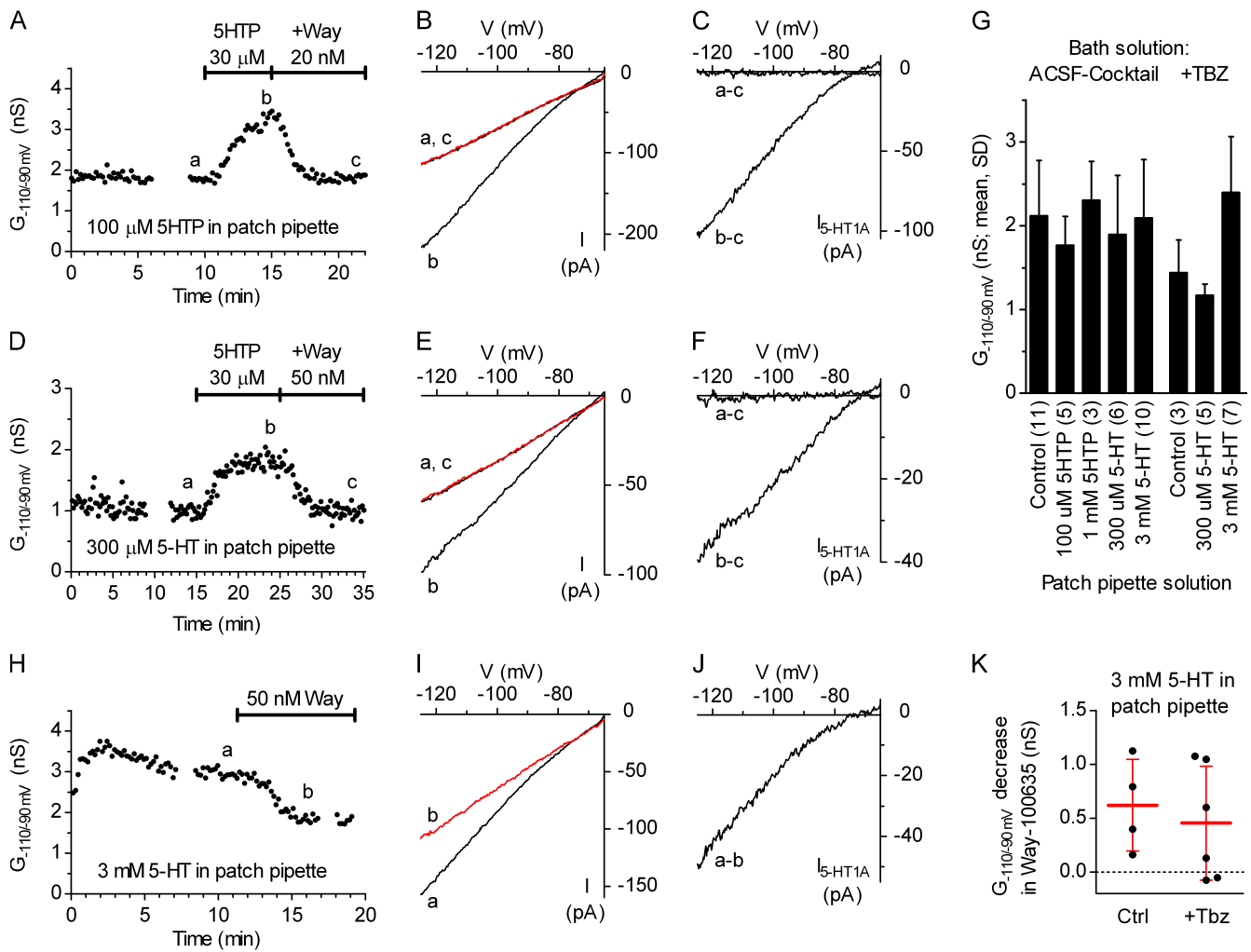
Figure 10. Efflux of 5-HT from a serotonergic neuron does not contribute significantly to its autoinhibition. (A) Time course of a representative experiment in which the pipette solution contained 100 µM 5HTP. Inwardly rectifying K⁺ conductance, determined from the slope of recorded current in the range from -110 to -90 mV ($G_{-110/-90mV}$) was constant during the first 10 min of the recording. Bath application of 30 µM 5HTP, indicated by the horizontal bar, produced a clear increase in $G_{-110/-90mV}$, which was completely reversed by the subsequent addition of Way-100635 (+Way). Interruptions in data correspond to passage into current-clamp mode for electrophysiological identification of the recorded neuron (see Materials and methods). (B) Current–voltage plot shows inwardly rectifying K⁺ currents of the same experiment recorded before (a) and after (b) bath application of 5HTP, and after the coapplication of 5HTP and Way-100635 (c; red trace). Traces are averages of the last six individual ramps recorded in the indicated conditions. (C) Current–voltage plot obtained by subtraction of Way-100635–insensitive current shows lack of 5-HT1A autoreceptor-activated GIRK current activation by intracellularly applied 5HTP and prominent activation by the bath application. (D) Time course of a representative experiment in which the pipette solution contained 300 nM 5-HT. Bath solution contained 10 µM Tbz. Horizontal bars indicate bath application of 5HTP and coapplication of 5HTP and Way-100635 (+Way). (E) Current–voltage plot of experiment shown in D. Traces are averages of 15 individual ramps. (F) Current–voltage plot obtained by subtraction of Way-100635–insensitive current shows lack of 5-HT1A autoreceptor-activated GIRK current (I_{5-HT1A}) activation by intracellularly applied 5-HT and its activation by the bath application of 30 µM 5HTP. (G) Histogram summarizing the effect of the intracellular application of 5-HT or 5HTP on the baseline $G_{-110/-90mV}$, measured at steady state, 10–15 min after establishing whole-cell configuration. The two-tailed Kruskal–Wallis test indicated a significant difference (P = 0.0105), but the only significant difference was between 300 µM 5-HT in Tbz and 3 mM 5-HT in Tbz groups (P < 0.01; Dunn's multiple comparison post-hoc test). (H) Time course of a representative experiment with 3 mM 5-HT in the pipette and bath application of Way-100635 (Way). (I) Current–voltage plot of experiment shown in H. Traces are averages of 12 individual ramps. (J) Current–voltage plot of the net Way-100635–sensitive current. (K) Scatter plot summarizing the magnitude of Way-100635–sensitive current in experiments with 3 mM 5-HT in the pipette and bath solution containing ACSF cocktail (Ctrl) or ACSF cocktail plus 10 µM Tbz (+Tbz). Bars correspond to mean ± SD. The decrease in inwardly rectifying K⁺ conductance by Way-100635 did not reach significance in individual groups (P = 0.063 and 0.078; one-tailed Wilcoxon matched-pairs test), whereas the analysis of pooled data indicated a significant decrease (P = 0.0034; one-tailed paired *t* test; normal distribution; P = 0.19; D'Agostino and Pearson omnibus test).

of 5-HT normally present in the cytosol is unknown, we used 5-HT at concentrations of 0.3 and 3 mM, assumed to be one to two orders of magnitude higher than normal, based on the rationale explained in Materials and methods. Similarly, 5HTP was applied at 0.1 and 1 mM, concentrations expected to partially and nearly completely saturate AADC in the recorded neuron, given that AADC K_m for 5HTP is $\sim$18–66 µM (Rahman et al., 1981; Jebai et al., 1997). In these experiments, after establishment of gigaseal, the cell-attached configuration was typically maintained for 5–7 min before rupturing the patch to allow for washout of 5-HT or 5HTP, which leaked out from the pipette tip. Loading of the recording neuron with 0.1 or 1 mM 5HTP (e.g., Fig. 10, A–C) or 300 µM 5-HT (e.g., Fig. 10, D–F) did not produce a detectable increase in inwardly rectifying K^+ conductance, which was however reliably induced in the same experiments by bath perfusion with 30 µM 5HTP, suggesting that 5-HT_o originated primarily from surrounding serotonergic neurons. In a subgroup of experiments with 5-HT loading, the bath solution also contained 10 µM Tbz. A comparison of baseline inwardly rectifying K^+ conductance, recorded 10–15 min after establishing the whole-cell configuration to ensure thorough loading of the recorded neuron and complete washout of 5HTP or 5-HT leaked from the pipette before establishing gigaseal, did not reveal significantly increased intracellular 5HTP or 5-HT (Fig. 10 G). A small efflux of 5-HT from serotonergic neurons was revealed only in experiments in which the patch pipette contained a high (3 mM) 5-HT concentration, and in which, after a stable $G_{-110/-90\text{mV}}$ baseline, the addition of Way-100635 decreased $G_{-110/-90\text{mV}}$ (Fig. 10, H–K). Again, similar results were obtained regardless of the presence of Tbz, consistent with the nonvesicular nature of 5-HT release. An analysis of pooled data revealed that when a cell is loaded with 3 mM 5-HT, the application of Way-100635 decreased inwardly rectifying K^+ conductance by 0.52 ± 0.47 nS (mean $\pm$ SD; $n = 10$; P = 0.0034; one-tailed paired t test), revealing an efflux of 5-HT under these conditions.

Experiments involving intracellular application of 5-HT and 5HTP suggested that efflux of cytosolic 5-HT from a given serotonergic neuron does not contribute significantly to the autoinhibition of that neuron. However, these findings might have been influenced by SERT activity in two opposing ways. First, it is possible that 5-HT efflux from a 5HTP- or 5-HT–loaded neuron remained undetected, i.e., did not produce measurable GIRK channel activation caused by the concurrent removal of 5-HT_o by SERT located on surrounding serotonergic neurons. Second, it is possible that after the loading of a neuron with 3 mM 5-HT, the efflux of 5-HT responsible for 5-HT1A autoreceptor-mediated GIRK channel activation is in some part caused by SERT reversal. It was not feasible to test for this by doing experiments in the

presence of a SERT inhibitor, as that would not discriminate if 5-HT originated from the patched or from surrounding neurons. To overcome these limitations, experiments were done on raphe slices obtained from Tph2 knockout ($\text{Tph2}^{-/-}$) mice. To examine if there is detectable 5-HT release from a loaded neuron when SERT is inhibited, we loaded 3 mM 5-HT in serotonergic neurons of $\text{Tph2}^{-/-}$ mice and compared GIRK conductance in the presence of 1 µM citalopram and after the application of 50 nM Way-100635 (Fig. 11). The citalopram application itself did not significantly change inwardly rectifying K^+ conductance (0.55 ± 1.14 nS; mean $\pm$ SD; $n = 6$; P = 0.56; two-tailed Wilcoxon matched pairs test), and variable responses were observed in individual experiments, comprising both increase and decrease (e.g., Fig. 11, A and E; range of -0.38 to 2.28 nS), consistent with the dual effect of SERT inhibition on both 5-HT efflux from the loaded neuron through reverse transport and the uptake in surrounding neurons. In 3 mM 5-HT–loaded serotonergic neurons from $\text{Tph2}^{-/-}$ mice, inhibition of 5-HT1A autoreceptors by the addition of Way-100635 in the continuous presence of citalopram decreased inwardly rectifying K^+ conductance by 1.69 ± 0.90 nS (mean $\pm$ SD; $n = 8$; P = 0.0006; one-tailed paired t test; normal distribution; P = 0.68; D'Agostino and Pearson omnibus test) revealing a SERT-independent release of 5-HT from a single serotonergic neuron. Because these recordings were done in the synaptic blocker cocktail and recorded neurons were held at -65 mV, the release was occurring in the absence of firing activity. In addition, there was no change in GIRK conductance even in response to sustained firing induced by current injections in current clamp ($n = 6$; not depicted), further supporting the nonexocytotic origin of 5-HT_o.

As to whether cytosolic 5-HT efflux from a serotonergic neuron contributes to its autoinhibition, experimental results in slices obtained from $\text{Tph2}^{-/-}$ mice were similar to those observed in the rat. In $\text{Tph2}^{-/-}$ mice, a bath perfusion of 30 µM 5HTP produced more substantial activation of GIRK channels than cell loading with a much higher concentration of 5HTP or 5-HT (e.g., Fig. 11 E; representative of three experiments). In recordings in which the pipette solution contained 1 mM 5HTP, aiming to maximally induce 5-HT synthesis in the recorded cell, the leakage of 5HTP from the pipette tip before the gigaseal formation produced notable GIRK current at the beginning of whole-cell recording, which then faded away completely over the course of the recording (Fig. 11, F and G; representative of four experiments), suggesting the interneuronal nature of autoinhibition.

Firing suppression is mediated by 5-HT release from surrounding neurites

Finally, because findings of whole-cell experiments indicated that 5-HT_o underlying autoinhibition of a given serotonergic neuron originates principally in surrounding

serotonergic neurons, we wanted to confirm that the same holds true for the suppression of firing in intact serotonergic neurons in a more physiologically relevant setting. Thus, while recording the firing rate in the loose-seal cell-attached mode, Trp or 5HTP was focally applied to the slice at different lateral distances from the recorded neuron by using long-duration (3–6 min) pressure ejection with a picospritzer (Fig. 12). Focal application of 1 mM Trp 40–100 µm lateral of the recorded neuron suppressed firing comparable to (e.g., Fig. 12, A and B; $n = 3$) or stronger ($n = 2$) than the focal somatic application. Similar results were obtained with 1 mM 5HTP ($n = 3$; e.g., Fig. 12 C). Focal application by pressure ejection from the pipette positioned close to or directly over the recorded neuron cell body in most

cases interfered with the recording, causing a tissue displacement artifact and preventing a comparison of effects compared with distance. Spritzes into areas located ≥40 µm lateral to the recorded neuron were, however, reliable and permitted observation of the effect's time course. Spritzes of 1 mM Trp into areas largely devoid of cell bodies, located 40–50 µm lateral to the recorded neuron, after a lag of ∼20 s, rapidly suppressed the firing rate (Fig. 12 D), indicating that [5-HT]$_o$ concentration in the DRN is tightly controlled by the cytosolic 5-HT concentration in surrounding serotonergic dendrites and/or axons.

To alternatively achieve focal 5-HT precursor delivery to the cell body of recorded neuron without pressure ejection, we did a series of experiments in which loose-seal
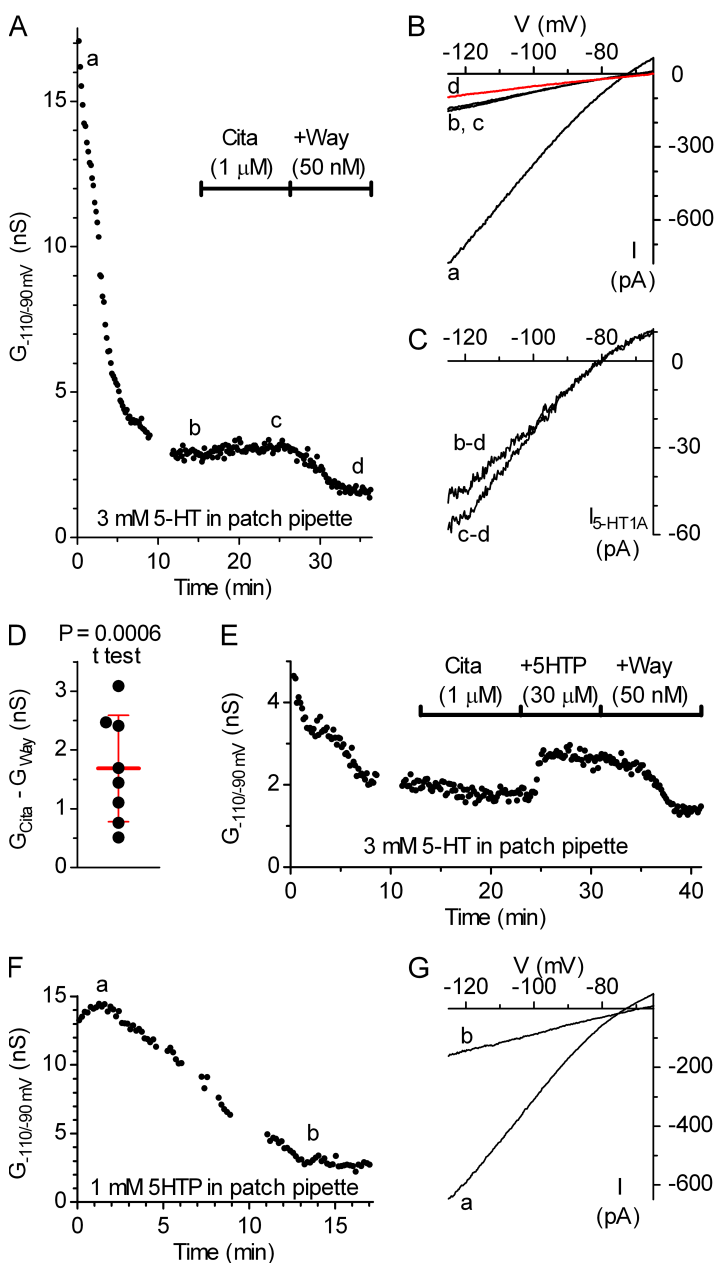

Figure 11. The effect of 5-HT efflux from a single neuron in slices obtained from Tph2$^{-/-}$ mice. (A) Time course of a representative experiment with 3 mM 5-HT in the pipette solution and bath application of 1 µM citalopram (Cita), followed by coapplication of 1 µM citalopram and 50 nM Way-100635 (+Way). Inwardly rectifying K$^+$ conductance (G$_{-110/-90mV}$) was determined from the slope of recorded current in range from -110 to -90 mV. Notable G$_{-110/-90mV}$ decaying during the first 10 min of the recording was caused by the activation of 5-HT1A autoreceptors, caused by the leakage of 5-HT from the pipette tip before the formation of gigaseal. (B) Current–voltage plot shows inwardly rectifying K$^+$ currents of the same experiment recorded after establishing whole-cell configuration (a), at the steady-state level before citalopram application (b), in citalopram (c), and in citalopram plus Way-100635 (d; red trace). Traces represent averages of three (a) or six individual ramps (b–d). (C) Current–voltage plot obtained by subtraction of Way-100635–insensitive current. (D) Scatter plot of magnitude of Way-100635–sensitive conductance in the presence of citalopram in experiments with 3 mM 5-HT in the pipette. Bars correspond to mean ± SD. (E) Time course of an experiment showing the effects of 3 mM 5-HT in the pipette and bath applications of citalopram (Cita), citalopram and 5HTP (+5HTP), and the addition of Way-100635 (+Way), suggesting that 5-HT$_o$ originates primarily from surrounding neurons. (F) Time course of a representative experiment in which the pipette solution containing 1 mM 5HTP shows marked inwardly rectifying K$^+$ current at the beginning of the recording, which faded away over the course of the recording. (G) Current–voltage plot of experiment shown in F. Traces are averages of six individual ramps recorded during the 2nd and the 14th min, respectively.

cell-attached recording was done with pipettes containing 1 mM Trp or 5HTP (Fig. 12 E). In these experiments, pipettes had a large-bore tip (R_{pip} of ≈1.7–2.1 MΩ) to increase the contact area with the recorded neuron. Contrary to spritz experiments, the firing rate was not suppressed by 5-HT precursors and, in experiments with 5HTP in the recording pipette solution, the firing rate was actually increasing during the first 2–5 min of recording, indicative of the 5HTP leakage out of the pipette before establishing loose-seal configuration.
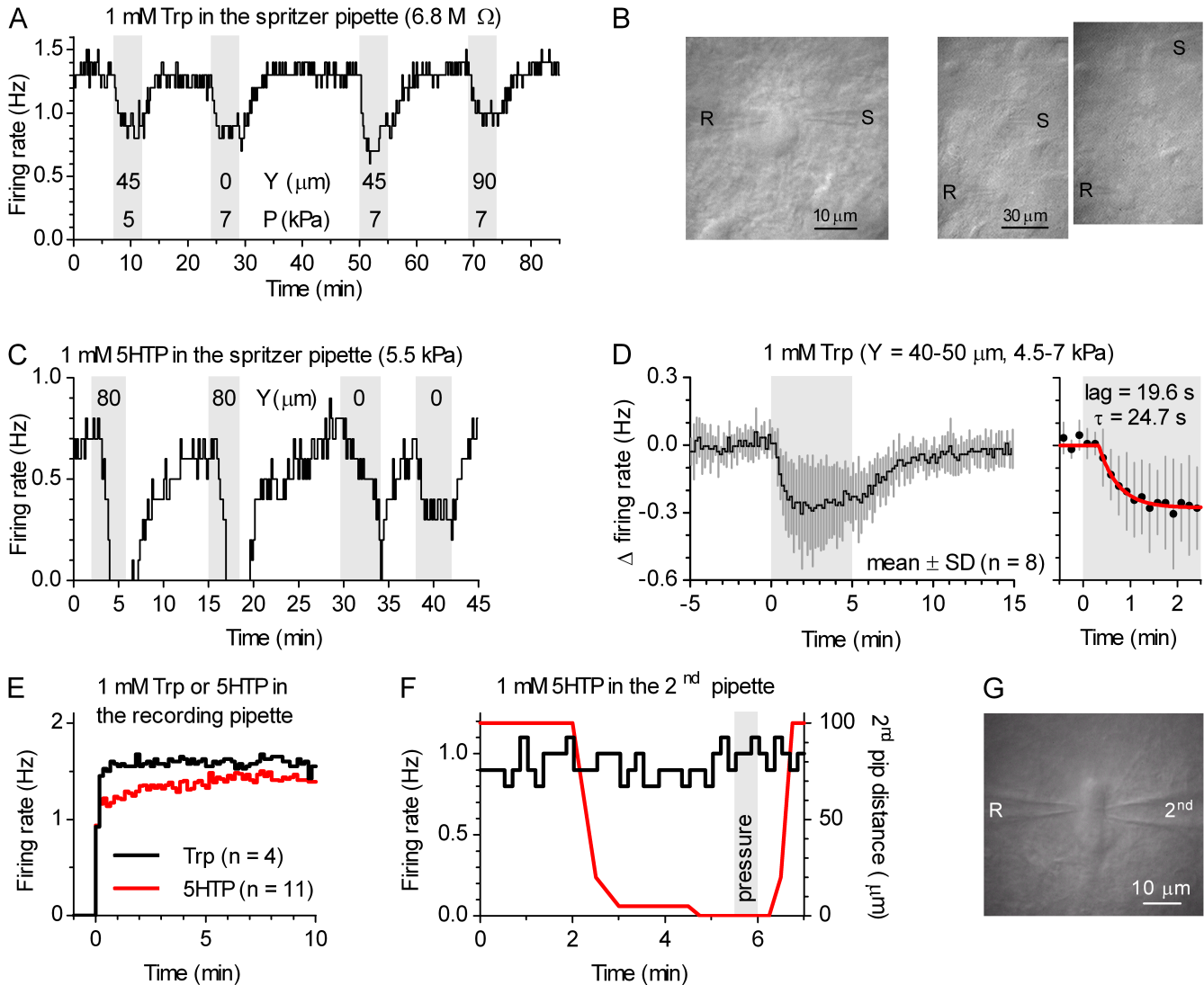
Figure 12. 5-HT–mediating suppression of firing originates in surrounding neurites. (A) Time course of representative experiment in which 1 mM Trp was spritzed 45 µm lateral, 90 µm lateral and directly toward the recorded neuron. (B) Photographs showing recorded neuron, recording pipette (R), and spritz pipette (S) arrangement for the experiment shown in A. (C) Time course of a representative experiment in which 1 mM 5HTP was spritzed 80 µm lateral and directly toward the cell body of the recorded neuron. Transient decrease in the firing rate at the end of the cell body–directed pulses is an artifact of tissue movement. (D) Average time course for experiments in which 1 mM Trp was spritzed 40–50 µm lateral to the recorded neuron ($n = 8$). Symbols represent the mean ± SD of the normalized, binned firing rate, expressed as absolute difference in the baseline firing rate computed over the 5 min preceding Trp application in each experiment. Shaded area corresponds to the spritz duration. Right, the onset of Trp-induced change on an enlarged scale. Red curve is a data fit of means with the function of the form Y = {0, if t < lag; $Y_{Trp}(-1 + e^{-(t - lag)/\tau})$, if t ≥ lag}, where lag is time from the application of Trp to the beginning of change, τ is the exponential time constant, and Y_{Trp} is the change in firing rate when steady-state level is achieved (lag = 19.6 s; 13.8–25.3 s 95% C.I.; τ = 24.7 s; 17.7–40.8 s 95% C.I.; Y_{Trp} = 0.27 Hz; 0.26–0.29 Hz 95% C.I. Hz; R^2 = 0.969). (E–G) Direct somatic application of Trp and 5HTP with the recording pipette did not change the firing rate of the recorded serotonergic neuron. (E) Average time course for loose-seal cell-attached recordings in which 1 mM Trp or 1 mM 5HTP was included in the recording pipette solution. (F) Time course of an experiment in which the recorded neuron was rapidly approached with the second, nonrecording wide-tip patch pipette (R_{pip} = 1.9 MΩ) containing 1 mM 5HTP during recording with 5-HT precursor-free pipette solution. The red line represents the distance between tip of the pipette and the neuron. Positive pressure was applied to the 5HTP-containing pipette for 30 s, indicated by the shaded area. (G) Photograph of experiment in F taken during the period when both the recording (R) and the second (second) pipette were touching the recorded neuron.

The bath application of 50 nM Way-100635 at the end of these recordings did not change the firing rate ($n = 3$; not depicted). In a final series of experiments, during firing rate recording by using 5-HT precursor-free pipette solution, focal 5HTP application was achieved by rapidly advancing a second, 5HTP-containing pipette (1 mM) until it touched the recorded neuron soma (Fig. 12, F and G; representative of four experiments). Again, the firing rate was insensitive to focal somatic delivery of 5HTP. Collectively, these findings confirm those of the whole-cell recordings, which indicate the interneuronal nature of autoinhibition and suggest that 5-HT$_o$ in the DRN primarily originates from surrounding serotonergic neurites.

DISCUSSION

The mechanisms regulating basal [5-HT]$_o$ in serotonergic nuclei are important because they determine the extent of 5-HT1A autoreceptor-mediated autoinhibition and thus the activity of the entire serotonergic system. The concentration of 5-HT$_o$ present in the DRN reflects a dynamic equilibrium among 5-HT synthesis, degradation, vesicular storage, release, and uptake (Fig. 13). Inhibition of SERT-mediated uptake is sufficient to considerably elevate [5-HT]$_o$ in the DRN, indicating that the activity of SERT compensates for substantial continuous 5-HT release under physiological conditions. In this study, we aimed to identify the origin of basal 5-HT$_o$ in the DRN and the underlying mechanism of release.

A widely held assumption that 5-HT release from axonal collaterals supplies basal 5-HT$_o$ and causes autoinhibition (Albert et al., 2011; Altieri et al., 2013) is supported by early electrophysiological studies that revealed that serotonergic inhibitory postsynaptic potentials can be evoked in serotonergic neurons (Yoshimura and Higashi, 1985; Williams et al., 1988; Pan et al., 1989). Our data confirmed the existence of IPSP/C$_{5\text{-HT}}$ but also suggested that they are not a prominent feature of the DRN, as strong electrical stimulation of nearby ($\sim$200-µm) tissue, particularly in the rostral extension of the DRN, often failed to evoke IPSP/C$_{5\text{-HT}}$ in serotonergic neurons. In addition, evoked IPSC$_{5\text{-HT}}$ had rather
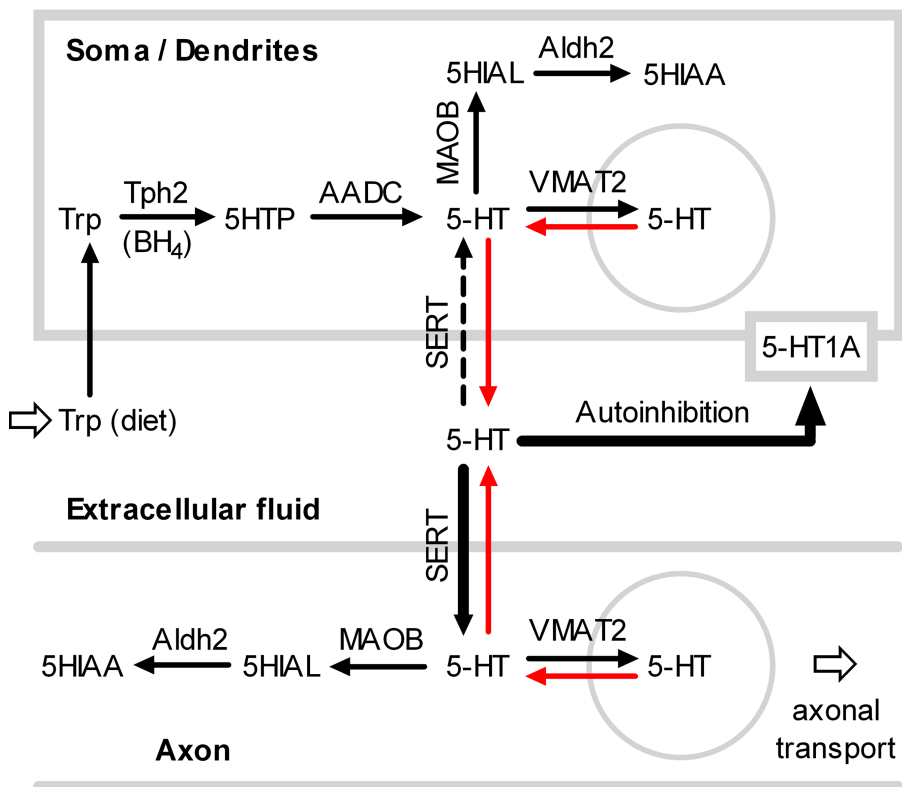

Figure 13. Schematic summary of metabolic and transmembrane 5-HT pathways in the DRN. In serotonergic cell bodies, 5-HT is synthesized de novo from Trp, an essential amino acid derived from food. Trp is converted to 5HTP by Tph2, the rate-limiting enzyme in 5-HT synthesis, which requires tetrahydrobiopterin (BH$_4$) as an essential cofactor. The intermediate metabolite 5HTP is rapidly converted to 5-HT by cytosolic AADC. Excessive cytosolic 5-HT is principally degraded by mitochondrial MAOB via conversion into 5-hydroxyindolealdehyde (5-HIAL), which is further converted into 5-hydroxyindoleacetic acid (5-HIAA) by aldehyde dehydrogenase type 2 (Aldh2). 5-HT is loaded from the cytosol into secretory vesicles by VMAT2. Vesicular 5-HT can be exocytotically released either in the proximity of cell bodies or, after the transport of vesicles along axons, in projection areas. Findings in this study indicate the existence of substantial nonexocytotic efflux of 5-HT across the plasma membrane, resulting in [5-HT]$_o$ sufficient to partially activate somatodendritic 5-HT1A autoreceptors. Extracellular 5-HT is taken back into serotonergic neurons by SERT, mostly into axons, where SERT is predominantly located (Tao-Cheng and Zhou, 1999). Red lines represent transmembrane flux of 5-HT down its concentration gradient.

small maximal amplitude values, with a median of $\sim$7 pA at the holding potential of -60 mV. These findings apparently contrast with previous studies reporting somewhat bigger responses, but the difference can be explained by less restrictive experimental conditions in previous studies. Namely, bigger responses could be, at least in part, attributed to the GABAB/GIRK-mediated synaptic transmission, as GABAB receptor antagonists were not used in early studies, and to multisynaptic mechanisms because, with the exception of the study by Pan et al. (1989), the recordings were done in the absence of any glutamate and GABA receptor antagonists. However, our findings are consistent with the anatomical evidence of scarce axonal 5-HT input in the DRN (Descarries et al., 1982), suggesting that relatively inconspicuous functional serotonergic synaptic transmission may be a general property in the DRN. In addition, given the paracrine characteristics of evoked serotonergic transmission (Bunin and Wightman, 1998; Bunin et al., 1998) and the abundance of SERT in the DRN (Qian et al., 1995), rapid removal of 5-HT_o by SERT conceivably contributes to the effects observed. Thus, although serotonergic synaptic transmission in the DRN could have a functional role, and in spite of the possibility that it is significantly reduced in slice preparation caused by the severing of serotonergic axons, the relative paucity of serotonergic synaptic transmission in the DRN supports our principal findings (see below), suggesting that conventional exocytotic 5-HT release is not required for the maintenance of basal $[5\text{-HT}]_o$.

We examined the mechanism of basal 5-HT release in the DRN by measuring the suppression of the serotonergic neuron firing rate in response to Trp challenge. To emulate in brain slice preparation the noradrenergic drive that during wakefulness exerts a maximal effect on serotonergic neuron firing (Levine and Jacobs, 1992), experiments were done in the presence of α_1 agonist phenylephrine. To reproduce the extent of autoinhibition matching that of the awake state, we used Trp at 30 µM, the concentration that restores 5-HT content in slices approximately to its level immediately after slicing (Mlinar et al., 2005). This concentration is in the range of Trp content in brain tissue, generally estimated to be 10–40 µM, although higher than that (6.7 µM) measured in the third ventricle cerebrospinal fluid in freely moving rat (Chaouloff et al., 1986). The extent of autoinhibition produced by 30 µM Trp in this study, on average $\sim$0.4 Hz or $\sim$25% reduction in the firing rate, is lower than that revealed by Way-100635 application in anesthetized rats, $\sim$0.9 Hz or $\sim$37–47% (Hajós et al., 2001; Haddjeri et al., 2004), and in awake cats, $\sim$1.2 Hz or 40% (Fornal et al., 1996). The weaker autoinhibition observed in slice preparations can be attributed to several factors such as: the presence of weak autoinhibition, even in the absence of Trp (Corradetti et al., 1996); weaker activity of tryptophan hydroxylase, mostly caused by a reduced level of its essential cofactor tetrahydrobiopterin (Sawada et al., 1986; Liu et al., 2005); and a decreased number of intact neurites from which 5-HT_o apparently originates. Nevertheless, the extent of firing suppression produced by Trp challenge was sufficient for the scope of this study, and because this effect of Trp is fully dependent on 5-HT1A autoreceptors and neuronal Tph2, we consider the Trp challenge to be an appropriate tool for studying the mechanisms regulating basal $[5\text{-HT}]_o$. We show that the firing suppression induced by 30 µM Trp is independent of GABA and glutamate transmission. Thus, although GABAergic (Liu et al., 2000; Tao and Auerbach, 2003) and glutamateric (De Kock et al., 2006; Colgan et al., 2012) transmission in the DRN can influence serotonergic neuron activity, they do not contribute to the autoinhibition. Similarly, 5-HT1A autoreceptor-mediated firing suppression induced by 30 µM Trp is not dependent on 5-HT accumulation in synaptic vesicles, indicating the cytosolic origin of 5-HT_o in the DRN. It is noteworthy that the increase in cytosolic 5-HT concentration, produced by Trp challenge, can cause an increase in $[5\text{-HT}]_o$ and thus autoinhibition not only by increasing the release rate but also by decreasing the reuptake rate caused by increased 5-HT gradient across the plasma membrane. Therefore, the $[5\text{-HT}]_o$ directly reflects the cytosolic 5-HT concentration and is largely independent of vesicular 5-HT. The release of 5-HT that maintains basal $[5\text{-HT}]_o$ can be detected under conditions of inhibited uptake. Thus, in experiments done in Trp-free ACSF, the block of SERT produced a marked suppression of firing, revealing substantial 5-HT release, even under conditions of subphysiological cytosolic 5-HT level. Marked suppression of firing by SERT block was also observed when 5-HT accumulation in synaptic vesicles was prevented by VMAT2 inhibition, confirming that the basal $[5\text{-HT}]_o$ is maintained by nonexocytotic 5-HT release.

Further characteristics of 5-HT release were revealed by using 5-HT1A autoreceptor-activated GIRK channels of patched serotonergic neurons as a sensor of 5-HT_o. In these experiments, the increase in $[5\text{-HT}]_o$ induced by the Trp challenge was at the limit of detection, but when unmasked under the SERT block, 30 µM of Trp-induced 5-HT release produced an increase in GIRK conductance of typically $\sim$1–3 nS, corresponding to an estimated increase in $[5\text{-HT}]_o$ of $\sim$30–90 nM. These experiments reveal that the firing activity is not required for the underlying release and confirm the presence of considerable basal nonexocytotic 5-HT release in the DRN. We also show that the increase in $[5\text{-HT}]_o$ produced via SERT block by SSRI citalopram, apart from higher magnitude, has properties comparable to the increase induced by Trp challenge. Thus, we observed a prominent citalopram-induced increase in GIRK conductance both under basal conditions and under conditions

of abolished firing activity, Ca^{2+} influx and 5-HT accumulation in synaptic vesicles. These findings indicate that not only basal $[5\text{-HT}]_o$ but also elevated $[5\text{-HT}]_o$ induced by SSRI antidepressant treatment are maintained by an activity-independent nonexocytotic mechanism. This conclusion is further supported by experiments in which the endogenous 5-HT level was elevated by application of the intermediate 5-HT precursor, 5HTP, which can increase the rate of 5-HT synthesis above its physiological level, as the rate-limiting step in 5-HT synthesis is bypassed. Characteristics of 5HTP-induced autoinhibition were comparable with that induced by Trp, i.e., nonexocytotic and activity- and SERT-independent, indicating that in the DRN, 5-HT release under conditions of supraphysiological levels of endogenous 5-HT is mediated by the same mechanism as basal release.

Given the cytosolic origin of 5-HT_o, we examined the possibility that autoinhibition is caused by 5-HT_o originating in the autoinhibited neuron itself. Several findings of this study indicate that 5-HT_o underlying 5-HT1A autoreceptor-mediated autoinhibition does not originate in the autoinhibited neuron but in surrounding serotonergic neurons and/or serotonergic neurites that permeate the DRN. First, whole-cell recordings in which high concentrations of 5-HT or 5-HTP are intracellularly applied by the recording pipette suggest that an individual serotonergic neuron can be only marginally autoinhibited by 5-HT originating in that neuron. Considering the possibility that intracellular loading did not maximally increase 5-HT in the most distal neurites, these experiments clearly show that at least somatic and perisomatic 5-HT efflux from a given neuron does not underlie its autoinhibition. Second, cell-attached recordings in which high concentrations of Trp or 5HTP are included in the recording pipette or in another, closely positioned pipette further suggest that the neuron does not inhibit itself. Third, cell-attached recordings in which Trp or 5HTP are applied by pressure ejection from a spritz pipette suggest that 5-HT originates in surrounding serotonergic neurons, primarily in the dense network of neurites surrounding serotonergic cell bodies.

The lack of dependence of autoinhibition on 5-HT accumulation in synaptic vesicles strongly suggests that exocytotic release is not required for the supply of 5-HT_o in the DRN. It would still be possible that even under conditions of inhibited VMAT2 or V-ATPase, recycling of vesicles with residual 5-HT can to some extent suppress firing and activate GIRK channels. However, no indications of such a mechanism were observed. For example, regardless of whether 5-HT accumulation in secretory vesicles is inhibited or not, the magnitude and the kinetics of the GIRK conductance activation upon citalopram or Trp application are similar. Having excluded vesicular 5-HT pool as the source of 5-HT_o in the DRN, potential release mechanisms from the cytosolic pool were considered. The leakage of 5-HT from neurons damaged during slice preparation is unlikely because recordings were done on neurons located ≥40 µm from the slice surface, and 5-HT precursors as well as SERT blockers produce weaker effects in superficial neurons (Mlinar et al., 2005), the opposite of what would occur if 5-HT leaked out of damaged neurons. Next, the possibility that the release of cytosolic 5-HT occurs by reversal of SERT transport can be ruled out because 5-HT efflux persists in the presence of saturating concentration of citalopram. That SERT is not required for the release is also suggested by the finding that the application of 5-HT precursors suppresses firing of serotonergic neurons in slices obtained from SERT knockout ($Sert^{-/-}$) mice comparable to that from control animals (Araragi et al., 2013). Another potential nonexocytotic 5-HT release mechanism is through polyspecific organic cation transporters, such as organic cation transporters 1–3 and plasma membrane monoamine transporter, which have affinity for 5-HT in micromolar to low millimolar range and are able to translocate 5-HT across the plasma membrane in either direction (Engel et al., 2004; Amphoux et al., 2006; Koepsell et al., 2007). However, none of these transporters seems to be consistently expressed in serotonergic neurons. 5-HT could also potentially leak out of the cytosol through a large cation channel, e.g., through connexin or pannexin hemichannels. To our knowledge, no such channel is expressed in DRN serotonergic neurons.

Finally, 5-HT could cross the plasma membrane by passive diffusion, a mechanism generally assumed as improbable in underlying 5-HT release (Hensler, 2012), given that at physiological pH, 5-HT is predominately in its protonated form (5-HTH^+), and charged molecules do not easily partition the membrane. However, it has recently been shown (Peters et al., 2013) that, unusually for a hydrophilic solute, 5-HT partitions strongly in lipid bilayers, having a distribution coefficient (D_x or $P_{app,x}$ of ≈1,200 for dimyristoylphosphatidylcholine bilayers; in mole fraction units) comparable to that of highly hydrophobic compounds, ~100 times higher than the partitioning coefficient of neutral 5-HT form for bulk lipid–water mixtures (P_x 0f ≈10.8 for octanol–water mixtures), and $>10^5$ times higher than that of protonated 5-HT ($P_{\text{"true"},x}$ of ≈0.04 for water–nitrobenzene interface; Tatsumi and Ueda, 2011). Consistently, the hypothesis that simple diffusion could underlie 5-HT release in the DRN is further supported by the observation that diffusion of 5-HT from phosphatidylcholine vesicles occurs with the mean lifetime (or time constant, τ) of ~70 s and the permeability coefficient of ~4.8×10^{-8} cm s^{-1} (Berry et al., 2013). Although passive diffusion of 5-HT across the plasma membrane has not been shown in serotonergic neurons, it has been demonstrated

in nonexcitable cells (Erickson et al., 1992; Scholze et al., 2000; Sitte et al., 2000). Based on the pH dependence, it appears that 5-HT crosses the plasma membrane in its neutral form (Erickson et al., 1992). The efflux of 5-HT by passive diffusion from preloaded HEK 293 cells was determined to occur with the fractional release of $\sim$1.2–1.5% min^{-1}, corresponding to the τ of $\sim$64–78 min (Scholze et al., 2000, 2001). Here, by using 5-HT1A autoreceptor-activated GIRK channels as a 5-HT$_o$ sensor, we estimated the lower limit of nonexocytotic 5-HT release rate in the DRN. Under conditions of inhibited VMAT2 and SERT, bath application of Trp produced an increase in GIRK conductance with the time constant of 82.3–89.0 s. Even faster kinetics were observed in recordings of firing rate and focal application of Trp (τ = 26.7 s), but because 5-HT reuptake was not inhibited in these experiments, the kinetics could have been accelerated also via a SERT-dependent mechanism. A considerably higher 5-HT efflux rate observed here, compared with that found in HEK 293 cells, does not necessarily preclude diffusional efflux in the DRN. It is likely attributable to structural characteristics of serotonergic neurons, i.e., their long and thin dendrites and axons that substantially increase the plasma membrane surface over which 5-HT may diffuse. In addition, the DRN is a region with the greatest density of SERT in the brain, and serotonergic cell bodies are surrounded by a dense network of SERT-immunoreactive neurites (Qian et al., 1995). It is reasonable to assume that the high surface/volume ratio of thin 5-HT neuron neurites in combination with a high transmembrane gradient of 5-HT generated by SERT and 5-HT synthesis provide a basis for significant passive 5-HT efflux in the DRN. Thus, although transporter- and channel-mediated mechanisms cannot be fully ruled out, we suggest that continuous release of 5-HT in the DRN may be mediated by simple diffusion of 5-HT across the plasma membrane.

Given the substantial efflux of cytosolic 5-HT in the presence of a large transmembrane 5-HT gradient, the passive efflux of 5-HT could also occur from SERT-expressing axons in projection areas. Consistent with this hypothesis, SERT-independent 5-HT release was observed in rat hippocampal slices after the application of 5-HT–releasing amphetamine analogues as well as after the inhibition of VMAT2 (Mlinar and Corradetti, 2003), whereas nonvesicular 5-HT release with an unidentified mechanism was shown from synaptosomes obtained from mice in which the VMAT2 gene was deleted in serotonergic neurons (Narboux-Nême et al., 2011). Passive 5-HT efflux possibly also occurs in axons of neurons that transiently express SERT during development, such as thalamocortical neurons (Persico et al., 2001). Furthermore, a physiologically relevant passive efflux of transmitter might not be limited to 5-HT. Similar to our findings, substantial passive "leakage" of acetylcholine

has been shown at the neuromuscular junction under resting conditions (Katz and Miledi, 1977). Importantly, passive diffusion across the plasma membrane of intact cells has been shown for other monoamine transmitters, e.g., dopamine (Kim et al., 2000; Scholze et al., 2001), and efflux of dopamine and especially noradrenaline from phosphatidycholine vesicles has been shown to occur at a higher rate compared with 5-HT (Berry et al., 2013). As all monoamine transmitters have a high transmembrane gradient established by respective high affinity plasma membrane transporters, it can be hypothesized that simple diffusion of monoamine transmitters across the plasma membrane may be a significant component of their release. In particular, because brain monoamine systems are under regulatory control by negative feedback analogous to that of serotonergic system, and because monoaminergic nuclei characteristically contain a network of monoaminergic neurites, it is possible that transmembrane diffusion contributes to autoinhibition of monoaminergic neurons in general.

Autoinhibitory regulation of the serotonergic system at the level of serotonergic nuclei has remained unclear in spite of numerous studies investigating the function of the key proteins involved, 5-HT1A autoreceptors and SERT. Our data suggest that [5-HT]$_o$ in the DRN primarily reflect cytosolic 5-HT concentrations in neurites of serotonergic neurons, revealing some interesting properties of the serotonergic system when considered in light of structural organization of serotonergic nuclei. Thus, as 5-HT synthesizing enzymes, Tph2 and AADC, are present throughout the cytosol of serotonergic neurons (Joh et al., 1975), and Tph2, contrary to 5-HT, is more abundant in cell bodies than in projection areas (Weissmann et al., 1987), and while SERT is expressed abundantly along axons, but at a low level on the somatodendritic plasma membrane (Tao-Cheng and Zhou, 1999), it can be hypothesized that newly synthesized 5-HT "leaks out" of somatodendritic regions into the extracellular space from where it is then taken up into the axons, resulting in an inverted flow of transmission of newly synthesized 5-HT compared with canonical synaptic transmission (see Fig. 13). A further consequence of axonal expression of SERT is generation of a large 5-HT gradient across axonal plasma membrane, suggesting that [5-HT]$_o$ can also originate in axons, as the leakage is proportional to the transmembrane gradient. Additional research is required to characterize the relative contribution of axonal and dendritic nonexocytotic 5-HT release in supplying 5-HT$_o$ in raphe nuclei.

Somewhat paradoxically, given the rapid forward transport of 5-HT–containing vesicles along axons, i.e., $\sim$50 μm min^{-1} in the axon of the giant cerebral neuron in Aplysia (Goldberg et al., 1976), the nonvesicular nature of 5-HT release in the DRN implies that the VMAT2-containing vesicles in serotonergic axons

surrounding serotonergic cell bodies function as a sink rather than a source of 5-HT_o. Substantial continuous "leakage" and reuptake of 5-HT indicate that serotonergic neurons share their 5-HT pool, i.e., 5-HT synthesized in one neuron can in significant amounts end up in other serotonergic neurons. Thus, SERT- and VMAT2-expressing neurons in the DRN could be fully functional 5-HT–releasing neurons, even if they are unable to synthesize 5-HT themselves.

Finally, our data suggest that the firing activity of an individual serotonergic neuron depends not only on its intrinsic electrical properties and 5-HT1A autoreceptor level but also on density and the arrangement of surrounding serotonergic neurons and their neurites. Together with the fact that the 5-HT pool is shared by serotonergic neurons, this indicates that the brain 5-HT system does not function as a sum of independently acting serotonergic neurons, but as a highly interdependent neuronal network. The morphology of 5-HT neuron dendritic arborization and axon collaterals in raphe nuclei may be a key factor in determining the extent of tonic activation of 5-HT1A autoreceptors and thus the activity of the entire brain 5-HT system. The relationship between serotonergic neurite structure and SERT and 5-HT1A autoreceptor expression may be crucial for the regulation of a variety of 5-HT–dependent physiological and behavioral processes, and its disruption may cause pathological conditions, such as depression and related disorders.

REFERENCES

Adams, S.V., and L.J. DeFelice. 2002. Flux coupling in the human serotonin transporter. *Biophys. J.* 83:3268–3282. http://dx.doi.org/10.1016/S0006-3495(02)75328-9

Adell, A., and F. Artigas. 1998. A microdialysis study of the in vivo release of 5-HT in the median raphe nucleus of the rat. *Br. J. Pharmacol.* 125:1361–1367. http://dx.doi.org/10.1038/sj.bjp.0702206

Adell, A., A. Carceller, and F. Artigas. 1993. In vivo brain dialysis study of the somatodendritic release of serotonin in the Raphe nuclei of the rat: Effects of 8-hydroxy-2-(di-*n*-propylamino)tetralin. *J. Neurochem.* 60:1673–1681. http://dx.doi.org/10.1111/j.1471-4159.1993.tb13390.x

Adell, A., P. Celada, M.T. Abellán, and F. Artigas. 2002. Origin and functional role of the extracellular serotonin in the midbrain raphe nuclei. *Brain Res. Brain Res. Rev.* 39:154–180. http://dx.doi.org/10.1016/S0165-0173(02)00182-0

Albert, P.R., B. Le François, and A.M. Millar. 2011. Transcriptional dysregulation of 5-HT1A autoreceptors in mental illness. *Mol. Brain.* 4:21. http://dx.doi.org/10.1186/1756-6606-4-21

Allers, K.A., and T. Sharp. 2003. Neurochemical and anatomical identification of fast- and slow-firing neurones in the rat dorsal raphe nucleus using juxtacellular labelling methods in vivo. *Neuroscience.* 122:193–204. http://dx.doi.org/10.1016/S0306-4522(03)00518-9

Altieri, S.C., A.L. Garcia-Garcia, E.D. Leonardo, and A.M. Andrews. 2013. Rethinking 5-HT1A receptors: Emerging modes of inhibitory feedback of relevance to emotion-related behavior. *ACS Chem. Neurosci.* 4:72–83. http://dx.doi.org/10.1021/cn3002174

Amphoux, A., V. Vialou, E. Drescher, M. Brüss, C. Mannoury La Cour, C. Rochat, M.J. Millan, B. Giros, H. Bönisch, and S. Gautron. 2006. Differential pharmacological in vitro properties of organic cation transporters and regional distribution in rat brain. *Neuropharmacology.* 50:941–952. http://dx.doi.org/10.1016/j.neuropharm.2006.01.005

Araragi, N., B. Mlinar, G. Baccini, L. Gutknecht, K.P. Lesch, and R. Corradetti. 2013. Conservation of 5-HT1A receptor-mediated autoinhibition of serotonin (5-HT) neurons in mice with altered 5-HT homeostasis. *Front. Pharmacol.* 4:97. http://dx.doi.org/10.3389/fphar.2013.00097

Artigas, F., L. Romero, C. de Montigny, and P. Blier. 1996. Acceleration of the effect of selected antidepressant drugs in major depression by 5-HT1A antagonists. *Trends Neurosci.* 19:378–383. http://dx.doi.org/10.1016/S0166-2236(96)10037-0

Audero, E., E. Coppi, B. Mlinar, T. Rossetti, A. Caprioli, M.A. Banchaabouchi, R. Corradetti, and C. Gross. 2008. Sporadic autonomic dysregulation and death associated with excessive serotonin autoinhibition. *Science.* 321:130–133. http://dx.doi.org/10.1126/science.1157871

Audero, E., B. Mlinar, G. Baccini, Z.K. Skachokova, R. Corradetti, and C. Gross. 2013. Suppression of serotonin neuron firing increases aggression in mice. *J. Neurosci.* 33:8678–8688. http://dx.doi.org/10.1523/JNEUROSCI.2067-12.2013

Baccini, G., B. Mlinar, E. Audero, C.T. Gross, and R. Corradetti. 2012. Impaired chemosensitivity of mouse dorsal raphe serotonergic neurons overexpressing serotonin 1A (Htr1a) receptors. *PLoS ONE.* 7:e45072. http://dx.doi.org/10.1371/journal.pone.0045072

Balaji, J., R. Desai, S.K. Kaushalya, M.J. Eaton, and S. Maiti. 2005. Quantitative measurement of serotonin synthesis and sequestration in individual live neuronal cells. *J. Neurochem.* 95:1217–1226. http://dx.doi.org/10.1111/j.1471-4159.2005.03489.x

Berry, M.D., M.R. Shitut, A. Almousa, J. Alcorn, and B. Tomberli. 2013. Membrane permeability of trace amines: Evidence for a regulated, activity-dependent, nonexocytotic, synaptic release. *Synapse.* 67:656–667. http://dx.doi.org/10.1002/syn.21670

Bosker, F., A. Klompmakers, and H. Westenberg. 1994. Extracellular 5-hydroxytryptamine in median raphe nucleus of the conscious rat is decreased by nanomolar concentrations of 8-hydroxy-2-(di-n-propyl-amino) tetralin and is sensitive to tetrodotoxin. *J. Neurochem.* 63:2165–2171. http://dx.doi.org/10.1046/j.1471-4159.1994.63062165.x

Bosker, F.J., T.Y. de Winter, A.A. Klompmakers, and H.G. Westenberg. 1996. Flesinoxan dose-dependently reduces extracellular 5-hydroxytryptamine (5-HT) in rat median raphe and dorsal hippocampus through activation of 5-HT1A receptors. *J. Neurochem.* 66:2546–2555. http://dx.doi.org/10.1046/j.1471-4159.1996.66062546.x

Bruns, D., D. Riedel, J. Klingauf, and R. Jahn. 2000. Quantal release of serotonin. *Neuron.* 28:205–220. http://dx.doi.org/10.1016/S0896-6273(00)00097-0

Bunin, M.A., and R.M. Wightman. 1998. Quantitative evaluation of 5-hydroxytryptamine (serotonin) neuronal release and uptake:

An investigation of extrasynaptic transmission. *J. Neurosci.* 18: 4854–4860.

Bunin, M.A., C. Prioleau, R.B. Mailman, and R.M. Wightman. 1998. Release and uptake rates of 5-hydroxytryptamine in the dorsal raphe and substantia nigra reticulata of the rat brain. *J. Neurochem.* 70:1077–1087. http://dx.doi.org/10.1046/j.1471-4159.1998.70031077.x

Chaouloff, F., D. Laude, Y. Guezennec, and J.L. Elghozi. 1986. Motor activity increases tryptophan, 5-hydroxyindoleacetic acid, and homovanillic acid in ventricular cerebrospinal fluid of the conscious rat. *J. Neurochem.* 46:1313–1316. http://dx.doi.org/10.1111/j.1471-4159.1986.tb00656.x

Chazal, G., and H.J. Ralston III. 1987. Serotonin-containing structures in the nucleus raphe dorsalis of the cat: An ultrastructural analysis of dendrites, presynaptic dendrites, and axon terminals. *J. Comp. Neurol.* 259:317–329. http://dx.doi.org/10.1002/cne .902590302

Colgan, L.A., I. Putzier, and E.S. Levitan. 2009. Activity-dependent vesicular monoamine transporter-mediated depletion of the nucleus supports somatic release by serotonin neurons. *J. Neurosci.* 29:15878–15887. http://dx.doi.org/10.1523/JNEUROSCI.4210-09.2009

Colgan, L.A., S.L. Cavolo, K.G. Commons, and E.S. Levitan. 2012. Action potential-independent and pharmacologically unique vesicular serotonin release from dendrites. *J. Neurosci.* 32:15737–15746. http://dx.doi.org/10.1523/JNEUROSCI.0020-12.2012

Cooper, M.A., K.E. McIntyre, and K.L. Huhman. 2008. Activation of 5-HT1A autoreceptors in the dorsal raphe nucleus reduces the behavioral consequences of social defeat. *Psychoneuroendocrinology.* 33:1236–1247. http://dx.doi.org/10.1016/j.psyneuen.2008.06.009

Corradetti, R., E. Le Poul, N. Laaris, M. Hamon, and L. Lanfumey. 1996. Electrophysiological effects of N-(2-(4-(2-methoxyphenyl)-1-piperazinyl)ethyl)-N-(2-pyridinyl)cyclohexane carboxamide (WAY 100635) on dorsal raphe serotonergic neurons and CA1 hippocampal pyramidal cells in vitro. *J. Pharmacol. Exp. Ther.* 278:679–688.

Crespi, F. 2009. Apamin increases 5-HT cell firing in raphe dorsalis and extracellular 5-HT levels in amygdala: A concomitant in vivo study in anesthetized rats. *Brain Res.* 1281:35–46. http://dx.doi .org/10.1016/j.brainres.2009.05.021

Crespi, F., K.F. Martin, and C.A. Marsden. 1988. Measurement of extracellular basal levels of serotonin in vivo using nafion-coated carbon fibre electrodes combined with differential pulse voltammetry. *Neuroscience.* 27:885–896. http://dx.doi.org/10.1016/0306-4522(88)90191-1

De Kock, C.P.J., L.N. Cornelisse, N. Burnashev, J.C. Lodder, A.J. Timmerman, J.J. Couey, H.D. Mansvelder, and A.B. Brussaard. 2006. NMDA receptors trigger neurosecretion of 5-HT within dorsal raphe nucleus of the rat in the absence of action potential firing. *J. Physiol.* 577:891–905. http://dx.doi.org/10.1113/jphysiol.2006.115311

Descarries, L., K.C. Watkins, S. Garcia, and A. Beaudet. 1982. The serotonin neurons in nucleus raphe dorsalis of adult rat: A light and electron microscope radioautographic study. *J. Comp. Neurol.* 207:239–254. http://dx.doi.org/10.1002/cne.902070305

Engel, K., M. Zhou, and J. Wang. 2004. Identification and characterization of a novel monoamine transporter in the human brain. *J. Biol. Chem.* 279:50042–50049. http://dx.doi.org/10.1074/jbc .M407913200

Erickson, J.D., L.E. Eiden, and B.J. Hoffman. 1992. Expression cloning of a reserpine-sensitive vesicular monoamine transporter. *Proc. Natl. Acad. Sci. USA.* 89:10993–10997. http://dx.doi.org/10.1073/pnas.89.22.10993

Evans, A.K., N. Reinders, K.A. Ashford, I.N. Christie, J.B. Wakerley, and C.A. Lowry. 2008. Evidence for serotonin synthesis-dependent regulation of in vitro neuronal firing rates in the midbrain

raphe complex. *Eur. J. Pharmacol.* 590:136–149. http://dx.doi .org/10.1016/j.ejphar.2008.06.014

Fakra, E., L.W. Hyde, A. Gorka, P.M. Fisher, K.E. Muñoz, M. Kimak, I. Halder, R.E. Ferrell, S.B. Manuck, and A.R. Hariri. 2009. Effects of HTR1A C(-1019)G on amygdala reactivity and trait anxiety. *Arch. Gen. Psychiatry.* 66:33–40. http://dx.doi.org/10.1001/archpsyc.66.1.33

Felten, D.L., and P. Harrigan. 1980. Dendrite bundles in nuclei raphe dorsalis and centralis superior of the rabbit: A possible substrate for local control of serotonergic neurons. *Neurosci. Lett.* 16:275–280. http://dx.doi.org/10.1016/0304-3940(80)90010-5

Fisher, P.M., C.C. Meltzer, S.K. Ziolko, J.C. Price, E.L. Moses-Kolko, S.L. Berga, and A.R. Hariri. 2006. Capacity for 5-HT1A-mediated autoregulation predicts amygdala reactivity. *Nat. Neurosci.* 9:1362–1363. http://dx.doi.org/10.1038/nn1780

Fornal, C.A., C.W. Metzler, R.A. Gallegos, S.C. Veasey, A.C. McCreary, and B.L. Jacobs. 1996. WAY-100635, a potent and selective 5-hydroxytryptamine$_{1A}$ antagonist, increases serotonergic neuronal activity in behaving cats: Comparison with (*S*)-WAY-100135. *J. Pharmacol. Exp. Ther.* 278:752–762.

Fowler, C.J., and K.F. Tipton. 1982. Deamination of 5-hydroxytryptamine by both forms of monoamine oxidase in the rat brain. *J. Neurochem.* 38:733–736. http://dx.doi.org/10.1111/j.1471-4159.1982.tb08692.x

Fuller, R.R., L.L. Moroz, R. Gillette, and J.V. Sweedler. 1998. Single neuron analysis by capillary electrophoresis with fluorescence spectroscopy. *Neuron.* 20:173–181. http://dx.doi.org/10.1016/S0896-6273(00)80446-8

Gallager, D.W., and G.K. Aghajanian. 1976. Inhibition of firing of raphe neurones by tryptophan and 5-hydroxytryptophan: Blockade by inhibiting serotonin synthesis with Ro-4-4602. *Neuropharmacology.* 15:149–156. http://dx.doi.org/10.1016/0028-3908(76)90023-X

Goldberg, D.J., J.E. Goldman, and J.H. Schwartz. 1976. Alterations in amounts and rates of serotonin transported in an axon of the giant cerebral neurone of *Aplysia californica*. *J. Physiol.* 259:473–490. http://dx.doi.org/10.1113/jphysiol.1976.sp011477

Gutknecht, L., N. Araragi, S. Merker, J. Waider, F.M. Sommerlandt, B. Mlinar, G. Baccini, U. Mayer, F. Proft, M. Hamon, et al. 2012. Impacts of brain serotonin deficiency following Tph2 inactivation on development and raphe neuron serotonergic specification. *PLoS ONE.* 7:e43157. http://dx.doi.org/10.1371/journal.pone .0043157

Haddjeri, N., N. Lavoie, and P. Blier. 2004. Electrophysiological evidence for the tonic activation of 5-HT(1A) autoreceptors in the rat dorsal raphe nucleus. *Neuropsychopharmacology.* 29:1800–1806. http://dx.doi.org/10.1038/sj.npp.1300489

Hajós, M., S.E. Gartside, A.E. Villa, and T. Sharp. 1995. Evidence for a repetitive (burst) firing pattern in a sub-population of 5-hydroxytryptamine neurons in the dorsal and median raphe nuclei of the rat. *Neuroscience.* 69:189–197. http://dx.doi.org/10 .1016/0306-4522(95)00227-A

Hajós, M., W.E. Hoffmann, I.V. Tetko, B. Hyland, T. Sharp, and A.E. Villa. 2001. Different tonic regulation of neuronal activity in the rat dorsal raphe and medial prefrontal cortex via 5-HT(1A) receptors. *Neurosci. Lett.* 304:129–132. http://dx.doi.org/10.1016/S0304-3940(01)01751-7

Hatcher, N.G., X. Zhang, J.N. Stuart, L.L. Moroz, J.V. Sweedler, and R. Gillette. 2008. 5-HT and 5-HT-SO4, but not tryptophan or 5-HIAA levels in single feeding neurons track animal hunger state. *J. Neurochem.* 104:1358–1363. http://dx.doi.org/10.1111/j.1471-4159.2007.05084.x

Hensler, J.G. 2012. Serotonin. *In* Basic Neurochemistry. Eighth edition. S.T. Brady, G.J. Siegel, R.W. Albers, and D.L. Price, editors. Academic Press, New York. 300–322. http://dx.doi.org/10.1016/B978-0-12-374947-5.00015-8

Hery, F., M. Faudon, and J.P. Ternaux. 1982. In vivo release of serotonin in two raphe nuclei (raphe dorsalis and magnus) of the cat. *Brain Res. Bull.* 8:123–129. http://dx.doi.org/10.1016/0361-9230(82)90038-7

Jacobs, B.L., and E.C. Azmitia. 1992. Structure and function of the brain serotonin system. *Physiol. Rev.* 72:165–229.

Jebai, F., N. Hanoun, M. Hamon, J. Thibault, G. Peltre, F. Gros, and M. Krieger. 1997. Expression, purification, and characterization of rat aromatic L-amino acid decarboxylase in *Escherichia coli. Protein Expr. Purif.* 11:185–194. http://dx.doi.org/10.1006/prep.1997.0778

Joh, T.H., T. Shikimi, V.M. Pickel, and D.J. Reis. 1975. Brain tryptophan hydroxylase: purification of, production of antibodies to, and cellular and ultrastructural localization in serotonergic neurons of rat midbrain. *Proc. Natl. Acad. Sci. USA.* 72:3575–3579. http://dx.doi.org/10.1073/pnas.72.9.3575

Katz, B., and R. Miledi. 1977. Transmitter leakage from motor nerve endings. *Proc. R. Soc. Lond. B Biol. Sci.* 196:59–72. http://dx.doi.org/10.1098/rspb.1977.0029

Kaushalya, S.K., R. Desai, S. Arumugam, H. Ghosh, J. Balaji, and S. Maiti. 2008. Three-photon microscopy shows that somatic release can be a quantitatively significant component of serotonergic neurotransmission in the mammalian brain. *J. Neurosci. Res.* 86:3469–3480. http://dx.doi.org/10.1002/jnr.21794

Kim, K.T., D.S. Koh, and B. Hille. 2000. Loading of oxidizable transmitters into secretory vesicles permits carbon-fiber amperometry. *J. Neurosci.* 20:RC101.

Koepsell, H., K. Lips, and C. Volk. 2007. Polyspecific organic cation transporters: Structure, function, physiological roles, and biopharmaceutical implications. *Pharm. Res.* 24:1227–1251. http://dx.doi.org/10.1007/s11095-007-9254-z

Levine, E.S., and B.L. Jacobs. 1992. Neurochemical afferents controlling the activity of serotonergic neurons in the dorsal raphe nucleus: Microiontophoretic studies in the awake cat. *J. Neurosci.* 12:4037–4044.

Li, Y.Q., H. Li, T. Kaneko, and N. Mizuno. 2001. Morphological features and electrophysiological properties of serotonergic and non-serotonergic projection neurons in the dorsal raphe nucleus: An intracellular recording and labeling study in rat brain slices. *Brain Res.* 900:110–118. http://dx.doi.org/10.1016/S0006-8993(01)02272-7

Liu, R., T. Jolas, and G. Aghajanian. 2000. Serotonin 5-HT(2) receptors activate local GABA inhibitory inputs to serotonergic neurons of the dorsal raphe nucleus. *Brain Res.* 873:34–45. http://dx.doi.org/10.1016/S0006-8993(00)02468-9

Liu, R.J., E.K. Lambe, and G.K. Aghajanian. 2005. Somatodendritic autoreceptor regulation of serotonergic neurons: dependence on L-tryptophan and tryptophan hydroxylase-activating kinases. *Eur. J. Neurosci.* 21:945–958. http://dx.doi.org/10.1111/j.1460-9568.2005.03930.x

Matos, F.F., C. Urban, and F.D. Yocca. 1996. Serotonin (5-HT) release in the dorsal raphé and ventral hippocampus: Raphé control of somatodendritic and terminal 5-HT release. *J. Neural Transm.* 103:173–190. http://dx.doi.org/10.1007/BF01292626

Mlinar, B., and R. Corradetti. 2003. Endogenous 5-HT, released by MDMA through serotonin transporter- and secretory vesicle-dependent mechanisms, reduces hippocampal excitatory synaptic transmission by preferential activation of 5-HT1B receptors located on CA1 pyramidal neurons. *Eur. J. Neurosci.* 18:1559–1571. http://dx.doi.org/10.1046/j.1460-9568.2003.02884.x

Mlinar, B., F. Tatini, C. Ballini, S. Nencioni, L. Della Corte, and R. Corradetti. 2005. Differential autoinhibition of 5-hydroxytryptamine neurons by 5-hydroxytryptamine in the dorsal raphe nucleus. *Neuroreport.* 16:1351–1355. http://dx.doi.org/10.1097/01.wnr.0000175249.25535.bf

Narboux-Nême, N., C. Sagné, S. Doly, S.L. Diaz, C.B. Martin, G. Angenard, M.P. Martres, B. Giros, M. Hamon, L. Lanfumey, et al. 2011. Severe serotonin depletion after conditional deletion of the vesicular monoamine transporter 2 gene in serotonin neurons: Neural and behavioral consequences. *Neuropsychopharmacology.* 36:2538–2550. http://dx.doi.org/10.1038/npp.2011.142

Pan, Z.Z., W.F. Colmers, and J.T. Williams. 1989. 5-HT-mediated synaptic potentials in the dorsal raphe nucleus: interactions with excitatory amino acid and GABA neurotransmission. *J. Neurophysiol.* 62:481–486.

Park, M.R., H. Imai, and S.T. Kitai. 1982. Morphology and intracellular responses of an identified dorsal raphe projection neuron. *Brain Res.* 240:321–326. http://dx.doi.org/10.1016/0006-8993(82)90227-X

Paxinos, G., and C. Watson. 1998. The Rat Brain in Stereotaxic Coordinates. Fourth edition. Academic Press, New York. 237 pp.

Penington, N.J., J.S. Kelly, and A.P. Fox. 1993. Whole-cell recordings of inwardly rectifying K$^+$ currents activated by 5-HT1A receptors on dorsal raphe neurones of the adult rat. *J. Physiol.* 469:387–405. http://dx.doi.org/10.1113/jphysiol.1993.sp019819

Persico, A.M., E. Mengual, R. Moessner, F.S. Hall, R.S. Revay, I. Sora, J. Arellano, J. DeFelipe, J.M. Gimenez-Amaya, M. Conciatori, et al. 2001. Barrel pattern formation requires serotonin uptake by thalamocortical afferents, and not vesicular monoamine release. *J. Neurosci.* 21:6862–6873.

Peters, G.H., C. Wang, N. Cruys-Bagger, G.F. Velardez, J.J. Madsen, and P. Westh. 2013. Binding of serotonin to lipid membranes. *J. Am. Chem. Soc.* 135:2164–2171. http://dx.doi.org/10.1021/ja306681d

Piñeyro, G., and P. Blier. 1999. Autoregulation of serotonin neurons: Role in antidepressant drug action. *Pharmacol. Rev.* 51:533–591.

Portas, C.M., M. Thakkar, D. Rainnie, and R.W. McCarley. 1996. Microdialysis perfusion of 8-hydroxy-2-(di-n-propylamino)tetralin (8-OH-DPAT) in the dorsal raphe nucleus decreases serotonin release and increases rapid eye movement sleep in the freely moving cat. *J. Neurosci.* 16:2820–2828.

Qian, Y., H.E. Melikian, D.B. Rye, A.I. Levey, and R.D. Blakely. 1995. Identification and characterization of antidepressant-sensitive serotonin transporter proteins using site-specific antibodies. *J. Neurosci.* 15:1261–1274.

Rahman, M.K., T. Nagatsu, and T. Kato. 1981. Aromatic L-amino acid decarboxylase activity in central and peripheral tissues and serum of rats with L-DOPA and L-5-hydroxytryptophan as substrates. *Biochem. Pharmacol.* 30:645–649. http://dx.doi.org/10.1016/0006-2952(81)90139-8

Riad, M., S. Garcia, K.C. Watkins, N. Jodoin, E. Doucet, X. Langlois, S. el Mestikawy, M. Hamon, and L. Descarries. 2000. Somatodendritic localization of 5-HT1A and preterminal axonal localization of 5-HT1B serotonin receptors in adult rat brain. *J. Comp. Neurol.* 417:181–194. http://dx.doi.org/10.1002/(SICI)1096-9861(20000207)417:2<181::AID-CNE4>3.0.CO;2-A

Richardson-Jones, J.W., C.P. Craige, B.P. Guiard, A. Stephen, K.L. Metzger, H.F. Kung, A.M. Gardier, A. Dranovsky, D.J. David, S.G. Beck, et al. 2010. 5-HT1A autoreceptor levels determine vulnerability to stress and response to antidepressants. *Neuron.* 65:40–52. http://dx.doi.org/10.1016/j.neuron.2009.12.003

Sawada, M., T. Sugimoto, S. Matsuura, and T. Nagatsu. 1986. (6R)-tetrahydrobiopterin increases the activity of tryptophan hydroxylase in rat raphe slices. *J. Neurochem.* 47:1544–1547. http://dx.doi.org/10.1111/j.1471-4159.1986.tb00792.x

Scholze, P., J. Zwach, A. Kattinger, C. Pifl, E.A. Singer, and H.H. Sitte. 2000. Transporter-mediated release: A superfusion study on human embryonic kidney cells stably expressing the human serotonin transporter. *J. Pharmacol. Exp. Ther.* 293:870–878.

Scholze, P., H.H. Sitte, and E.A. Singer. 2001. Substantial loss of substrate by diffusion during uptake in HEK-293 cells expressing

neurotransmitter transporters. *Neurosci. Lett.* 309:173–176. http://dx.doi.org/10.1016/S0304-3940(01)02058-4

Schuldiner, S., A. Shirvan, and M. Linial. 1995. Vesicular neurotransmitter transporters: from bacteria to humans. *Physiol. Rev.* 75:369–392.

Sharp, T., S.R. Bramwell, D. Clark, and D.G. Grahame-Smith. 1989. In vivo measurement of extracellular 5-hydroxytryptamine in hippocampus of the anaesthetized rat using microdialysis: Changes in relation to 5-hydroxytryptaminergic neuronal activity. *J. Neurochem.* 53:234–240. http://dx.doi.org/10.1111/j.1471-4159.1989.tb07319.x

Sitte, H.H., P. Scholze, P. Schloss, C. Pifl, and E.A. Singer. 2000. Characterization of carrier-mediated efflux in human embryonic kidney 293 cells stably expressing the rat serotonin transporter: A superfusion study. *J. Neurochem.* 74:1317–1324. http://dx.doi.org/10.1046/j.1471-4159.2000.741317.x

Tao, R., and S.B. Auerbach. 2003. Influence of inhibitory and excitatory inputs on serotonin efflux differs in the dorsal and median raphe nuclei. *Brain Res.* 961:109–120. http://dx.doi.org/10.1016/S0006-8993(02)03851-9

Tao, R., Z. Ma, and S.B. Auerbach. 1997. Influence of AMPA/kainate receptors on extracellular 5-hydroxytryptamine in rat midbrain raphe and forebrain. *Br. J. Pharmacol.* 121:1707–1715. http://dx.doi.org/10.1038/sj.bjp.0701292

Tao-Cheng, J.H., and F.C. Zhou. 1999. Differential polarization of serotonin transporters in axons versus soma-dendrites: an immunogold electron microscopy study. *Neuroscience.* 94:821–830. http://dx.doi.org/10.1016/S0306-4522(99)00373-5

Tatsumi, H., and T. Ueda. 2011. Ion transfer voltammetry of tryptamine, serotonin, and tryptophan at the nitrobenzene/water interface. *J. Electroanal. Chem.* 655:180–183. http://dx.doi.org/10.1016/j.jelechem.2011.02.011

Vandermaelen, C.P., and G.K. Aghajanian. 1983. Electrophysiological and pharmacological characterization of serotonergic dorsal raphe neurons recorded extracellularly and intracellularly in rat brain slices. *Brain Res.* 289:109–119. http://dx.doi.org/10.1016/0006-8993(83)90011-2

Wang, R.Y., and G.K. Aghajanian. 1982. Correlative firing patterns of serotonergic neurons in rat dorsal raphe nucleus. *J. Neurosci.* 2:11–16.

Weissmann, D., M.F. Belin, M. Aguera, C. Meunier, M. Maitre, C.D. Cash, M. Ehret, P. Mandel, and J.F. Pujol. 1987. Immunohistochemistry of tryptophan hydroxylase in the rat brain. *Neuroscience.* 23:291–304. http://dx.doi.org/10.1016/0306-4522(87)90290-9

Williams, J.T., W.F. Colmers, and Z.Z. Pan. 1988. Voltage- and ligand-activated inwardly rectifying currents in dorsal raphe neurons in vitro. *J. Neurosci.* 8:3499–3506.

Yoshimura, M., and H. Higashi. 1985. 5-Hydroxytryptamine mediates inhibitory postsynaptic potentials in rat dorsal raphe neurons. *Neurosci. Lett.* 53:69–74. http://dx.doi.org/10.1016/0304-3940(85)90099-0